Mathematical Biosciences 250 (2014) 54–68

Contents lists available at ScienceDirect

Mathematical Biosciences

journal homepage: www.elsevier.com/locate/mbs

Review

Physiologically-based modeling of sleep–wake regulatory networks

Victoria Booth [a,*], Cecilia G. Diniz Behn [b]

[a] Departments of Mathematics and Anesthesiology, University of Michigan, 530 Church Street, Ann Arbor, MI 48109-1043, United States
[b] Department of Applied Mathematics and Statistics, Colorado School of Mines, 1015 14th Street, Golden, CO 80401, United States

ARTICLE INFO

Article history:
Received 19 September 2013
Received in revised form 23 January 2014
Accepted 31 January 2014
Available online 11 February 2014

Keywords:
Sleep
Circadian rhythm
Firing rate models
Multiple timescales
Hysteresis
Bifurcation

ABSTRACT

Mathematical modeling has played a significant role in building our understanding of sleep–wake and circadian behavior. Over the past 40 years, phenomenological models, including the two-process model and oscillator models, helped frame experimental results and guide progress in understanding the interaction of homeostatic and circadian influences on sleep and understanding the generation of rapid eye movement sleep cycling. Recent advances in the clarification of the neural anatomy and physiology involved in the regulation of sleep and circadian rhythms have motivated the development of more detailed and physiologically-based mathematical models that extend the approach introduced by the classical reciprocal-interaction model. Using mathematical formalisms developed in the field of computational neuroscience to model neuronal population activity, these models investigate the dynamics of proposed conceptual models of sleep–wake regulatory networks with a focus on generating appropriate sleep and wake state transition patterns as well as simulating disease states and experimental protocols. In this review, we discuss several recent physiologically-based mathematical models of sleep–wake regulatory networks. We identify common features among these models in their network structures, model dynamics and approaches for model validation. We describe how the model analysis technique of fast–slow decomposition, which exploits the naturally occurring multiple timescales of sleep–wake behavior, can be applied to understand model dynamics in these networks. Our purpose in identifying commonalities among these models is to propel understanding of both the mathematical models and their underlying conceptual models, and focus directions for future experimental and theoretical work.

1. Introduction

The field of sleep research has a strong history of using mathematical models to frame understanding of sleep–wake cycling and circadian rhythms. As we all experience on a daily basis, these cycles are governed by the inevitable drive for sleep after periods of wakefulness and the circadian (∼24 h) rhythm propagated by the brain's suprachiasmatic nucleus (SCN). Within a sleep episode, additional rhythms occur in the transitions between rapid eye movement (REM) sleep and non-REM (NREM) or slow wave sleep with a period of approximately 90 min. These cyclic phenomena motivated the development of the classical mathematical models for sleep–wake regulation which include the two-process model for the timing of sleep based on the interaction of the homeostatic sleep drive and the circadian rhythm [1,2], coupled oscillator models for the same interactions [3,4] and the reciprocal interaction model for REM sleep cycling [5,6]. Although generally phenomenological in nature, each of these mathematical models had a significant impact on the field by formalizing conceptual models to guide experimental investigations and providing a context for interpreting experimental data.

Recent experimental results have clarified more of the anatomy and physiology underlying sleep–wake control. Most notably, identification of numerous brainstem and hypothalamic neuronal populations that have wake or sleep-promoting effects and elucidation of neurotransmitter-mediated interactions among these populations has led to the formulation of a putative regulatory network for the control of sleep and wake transitions. While experiments have established clear roles for some populations in such a network, such as the wake-promoting locus coeruleus (LC) and dorsal raphe (DR), the role of other populations, such as those involved in the regulation of REM sleep, are less clear. As described in more detail below, the classical reciprocal interaction hypothesis for REM sleep has been challenged by recent results implicating a role for mutually inhibitory interactions among neuronal populations with REM-promoting and REM-suppressing effects. However, consensus regarding the exact architecture of an inhibition-based REM regulatory network has not been reached,

* Corresponding author. Tel.: +1 734 763 4730.
E-mail addresses: vbooth@umich.edu (V. Booth), cdinizbe@mines.edu (C.G. Diniz Behn).

http://dx.doi.org/10.1016/j.mbs.2014.01.012
0025-5564/

and competing models for REM sleep regulation are vigorously debated.

Motivated by these recent results, mathematical models with a stronger physiological basis have been developed to provide quantitative underpinnings for the classical and more recent conceptual models of a sleep regulatory network [7–12]. Using a range of mathematical formalisms developed in the field of computational neuroscience to model neuronal population activity, these models investigate the dynamics of proposed conceptual models of sleep–wake regulatory networks with a focus on generating realistic sleep and wake state transition patterns and appropriate responses to simulated disease states and experimental protocols. To introduce these models, sample output from two recent sleep–wake network models is shown in Fig. 1. In Fig. 1A, the network model [13] simulates stereotypical human sleep where the hypnogram in the top trace summarizes the transitions in simulated behavioral state (wake, NREM sleep or REM sleep) dictated by the transitions in activity of the associated state-promoting neuronal populations shown in the lower traces (average firing rate (in Hz) of wake-promoting (f_W), NREM sleep-promoting (f_S) and REM sleep-promoting (f_R) neuronal populations). The model includes a homeostatic sleep drive variable (H), similar to Process S of the two-process model, that increases during wake and decreases during sleep to promote transitions between these two states. Additionally, the network accounts for the influence of the circadian rhythm on sleep–wake behavior by including input from the SCN (f_{SCN}) that varies on a 24 h time scale. In Fig. 1B, the sleep–wake network model [11,14] simulates typical rat sleep, as shown in the experimentally recorded hypnogram of rat sleep–wake behavior during the day (top trace). The highly variable nature of rat sleep is accounted for by including noise sources in the model. Below we discuss the anatomy and physiology that these and other recent sleep–wake network models are based on (Section 2) and the mathematical formalisms used to construct them (Section 4).

These recent physiological network models can play an important role in the scientific investigation of neuronal sleep–wake regulatory mechanisms because experimental investigations are uniquely limited by the fact that the outcome measurement, namely sleep–wake behavior, only exists in the intact animal. Key characteristics of the sleep or waking state have not been observed in reduced experimental preparations, such as brain slice, in situ preparation or culture of disassociated cells, which could permit close study of the time-varying activity of neuronal interactions. Thus, the experimental techniques available to probe neuronal regulatory mechanisms are limited to those that can be conducted in vivo without disrupting sleep, or post-mortem studies that can identify anatomy but not dynamic interactions. Physiologically-based mathematical models can bridge the gaps left by these limitations in experimental studies. In particular, numerous experimental groups have proposed schematics of conceptual network models and provided hypothetical descriptions of how network interactions could drive behavioral state transitions. However, these static conceptual models are not able to replicate time dynamics of transitions between sleep–wake states or to determine dynamic interactions inherent to network structure. Construction and analysis of mathematical models of these proposed networks can identify the dynamic interactions of constituent populations and neurotransmitters, and provide quantitative understanding of how network dynamics generate the temporal architecture of sleep–wake behavior. This architecture includes the timing, duration, and patterning of wake, NREM sleep, and REM sleep. Model analysis can identify limitations of different proposed network structures in accounting for various characteristics of sleep–wake regulation and can generate predictions suggesting

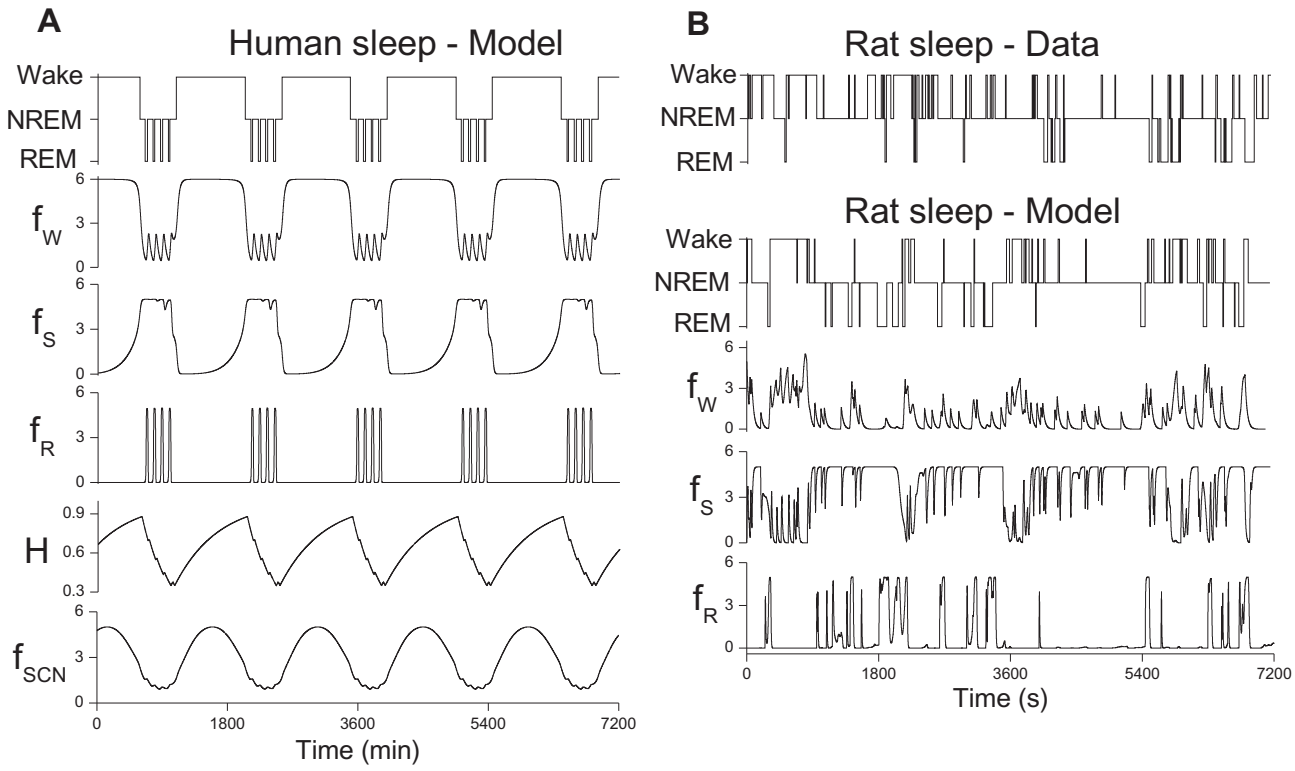

Fig. 1. Output of sleep–wake regulatory network models simulating stereotypical human sleep–wake behavior (A, [13]) and simulating typical rat sleep–wake behavior during the day (B, [11,14]) as shown in experimentally recorded rat behavior (B, top trace). Hypnograms (A, top trace; B, top two traces) summarize behavioral state changes over time and, in model outputs, are determined by the changes in average firing rates (in Hz) of wake-promoting (A, B: f_W), NREM sleep-promoting (A, B: f_S) and REM sleep-promoting (A, B: f_R) neuronal populations. A: the network model included influences of the homeostatic sleep drive (H) and the circadian rhythm propagated by the suprachiasmatic nucleus (f_{SCN}). B: to replicate the high variability of rat sleep, noise sources were included in the model. (rat sleep–wake behavioral data provided by George A. Mashour, University of Michigan).

how experimental approaches can refine our knowledge of the neurobiological control of sleep.

In this review, we discuss similarities and differences among several recent physiological models of sleep–wake regulatory networks [7–12]. At first glance, the differences among models outweigh the similarities since they use different mathematical formalisms, propose different network structures and focus on replicating sleep–wake behavior in different species and under different experimental conditions and disease states (see Table 1). However, the models share some important similarities in underlying network structures and model dynamics. We describe how the model analysis technique of fast–slow decomposition, which exploits the naturally occurring multiple timescales of sleep–wake behavior, can be applied to understand model dynamics in these networks. We also discuss approaches to model validation that can help to more tightly constrain these models and allow differentiation of the capabilities and limitations of each model.

The sleep–wake network models we focus on in this review reflect the general hypothesis of brainstem and hypothalamic control of sleep and wake states, in contrast to recent hypotheses of cortical control [15,16]. These models consist of specific network structures among wake and sleep-promoting neuronal populations that are motivated by recently proposed conceptual models of sleep regulation. Although sleep–wake behavior has been simulated by different types of models, including Markov models [17] and models that incorporate associations in dynamics among different behavioral states without assumptions on the generating mechanisms [18], we will focus on models with clear physiological correlates.

The paper is organized as follows. In the next section, we briefly review the anatomy and physiology of recently proposed conceptual networks for sleep–wake regulation. In Section 3 we review the classic phenomenological models for sleep–wake control. In Section 4, we describe the network structures and model formalisms of the recent physiological models of sleep–wake regulatory networks with a focus on identifying similarities among them. In Section 5, we use fast–slow decomposition to reveal the underlying dynamics of different model network structures. Finally, in Section 6, we discuss model validation approaches.

2. Physiology and anatomy

In the past 20 years, a focused effort to elucidate the anatomy and physiology of sleep–wake regulation has greatly contributed to our understanding of these processes. The identification of neuronal populations, particularly in the brainstem and hypothalamus, that are involved in sleep–wake regulation has led to the proposal of putative sleep–wake regulatory networks (for review see [19]). In these networks, neurotransmitter-mediated interactions among wake-, sleep-, and REM sleep-promoting populations control transitions between sleep and wake states. Proposed wake-promoting populations include LC, DR, and tuberomammilary nucleus (TMN), while proposed sleep-promoting populations include ventrolateral and medial preoptic areas (VLPO, mPOA). The evidence for mutually inhibitory projections between these wake- and sleep-promoting populations has given rise to the hypothesis of a sleep–wake "flip-flop switch" that drives rapid transitions between distinct states of wake and sleep [20]. By contrast, the mechanisms regulating REM sleep are less well-understood. In the 1970s, McCarley and Hobson proposed the reciprocal interaction hypothesis in which the excitatory cholinergic REM-promoting (REM-on) pontine populations laterodorsal and pedunculopontine tegmental nuclei (LDT/PPT) interact with the inhibitory monoaminergic wake-promoting population (LC) to regulate transitions between NREM and REM sleep [21]. More recent studies have suggested that multiple GABAergic populations play important roles in the control of REM sleep [22–27]. In particular, neuronal populations with REM-on activity profiles have been identified in the sublaterodorsal tegmental nucleus (SLD), portions of the ventrolateral periaqueductal gray matter (vlPAG), areas of the lateral hypothalamus (LH) and the dorsal paragigantocellular nucleus (DPGi). Identified neuronal groups with REM-suppressing (REM-off) activity profiles include other portions of the vlPAG and the dorsal part of the deep mesencephalic nucleus (dDPME). Based on these REM-associated neuronal groups and their synaptic interactions, alternative theories for the neuronal control of REM sleep have been proposed. In these conceptual models, GABA is the primary neurotransmitter, and mutually inhibitory synaptic interactions govern activity of these groups and thus transitions of REM sleep [19,26,28]. However, more evidence is necessary to reach a consensus regarding the exact architecture of a GABA-based REM regulatory network.

The 24 h timing of sleep–wake behavior across species has been well-documented, and experiments have shown that this timing is governed by the central circadian pacemaker in the SCN of the hypothalamus. The circadian variation of SCN electrical activity is associated with circadian modulation of sleep–wake behavior [29]. A distinct pattern of 24 h SCN neuronal firing, with generally higher firing rates during the light period and generally lower firing rates during the dark period, gives rise to the diversity of nocturnal, diurnal, and crepuscular behaviors observed across species [30–32]. However, there are subpopulations of SCN neurons with other firing profiles [33–35], and these may contribute to the

Table 1
Summary of recent physiological sleep–wake regulatory network models. In all models, transitions between NREM sleep and wake are mediated by mutual inhibition between NREM sleep- and wake-promoting neuronal populations.

Model	REM sleep hypothesis	Mathematical formalism	Modeled behaviors
Tamakawa et al. [7,76]	Reciprocal interaction	Firing rate	Rodent: basic sleep behavior; microinjection experiments; circadian modulation Human: basic sleep behavior
Diniz Behn et al. [8,77]	Reciprocal interaction	Morris–Lecar	Rodent: basic sleep behavior; role of orexin
Phillips and Robinson [9,69,70,73–75,81–85]	None	Firing rate	Human: basic sleep behavior; effects of: sleep deprivation, caffeine, fatigue, impulsive stimuli, internal desynchronization, shift work Mammalian: interspecies differences, unihemispheric sleep
Diniz Behn and Booth [11,13,14,78–80]	Reciprocal interaction	Firing rate & neurotransmitter	Rodent: basic sleep behavior; microinjection experiments; circadian modulation; temporal architecture of sleep patterns Human: basic sleep behavior; internal desynchronization
Rempe et al. [10]	Mutual inhibition	Morris–Lecar	Human: basic sleep patterns; sleep deprivation; role of orexin; sleep onset REM sleep
Kumar et al. [12]	Mutual inhibition	Morris–Lecar	Human: basic sleep patterns; sleep deprivation; role of orexin

complexity of observed behaviors and the flexibility and adaptability of circadian modulation [36].

Interestingly, the bidirectionality of projections that mediate interactions between the SCN and sleep–wake populations has only recently been appreciated. Both indirect and direct feedforward projections extend from the SCN to the sleep–wake network [37]; indirect projections are relayed through the subparaventricular zone (SPZ) and the dorsomedial hypothalamus (DMH) [36,38–40]. The majority of SCN neurons are GABAergic, but these feedforward projections are also mediated by glutamate and neuropeptides such as vasoactive intestinal peptide (VIP), vasopressin, gastrin-releasing peptide (GRP), somatostatin, and neuropeptide Y (NPY) [37,41–43] which may promote different behavioral states associated with differential timing of peak wakefulness [44–48]. Feedback projections from sleep–wake regulatory populations to the SCN provide a neuronal mechanism by which vigilance state can directly modulate activity of SCN neurons, and presumably the molecular circadian clock. In addition to the 24 h variation in SCN firing rate, experiments have established state-dependence in the firing of SCN neurons in which higher firing rates occur during wake and REM sleep states compared to NREM sleep states [49]; these changes are probably mediated through feedback projections from sleep–wake regulatory neuronal populations [50,51]. Furthermore, state-dependent behaviors such as seeking out a dark place for sleep and closing the eyes during sleep affect light input to the SCN and thus may provide a vigilance state-dependent modulation of SCN activity through the SCN's light sensitivity which is mediated by the melanopsin-sensitive light sensors in the eye (reviewed in [52]).

In addition to the circadian modulation of sleep–wake behavior, the timing and duration of sleep depend on the distribution of vigilance states in the preceding period, i.e., the propensity for sleep or wake increases with time spent in the other state. Borbély formalized this concept with the homeostatic sleep drive, "Process S," in the two-process model of sleep regulation [1,53]. Although there are probably many physiological mechanisms that contribute to this homeostatic modulation, the neuromodulator adenosine has been identified as one key component (reviewed in [54,55]). Extracellular adenosine concentrations in the basal forebrain and cortex increase with time in wakefulness [56], and microinjection experiments have established a somnogenic action of adenosine [57,58]. Adenosine may act on several neuronal populations involved in the sleep–wake regulatory network including LDT/PPT [59], basal forebrain [60–62], orexin neurons [63], and VLPO [64,65] [66]. The action of adenosine on the VLPO has been the key mechanism in model implementations of the homestatic sleep drive in sleep–wake regulatory networks, though some models have considered other sites of action as well [8].

Other neuronal populations have also been implicated in sleep–wake regulation, though they may not participate in an underlying core network. For example, orexin neurons in the lateral hypothalamus play a role in stabilizing and consolidating sleep–wake behavior, and dysregulation of the orexin system is associated with the sleep disorder narcolepsy (for review see [67]). Some models have included orexin neurons in their network structure and simulated sleep–wake behavior under different conditions of orexin activity [7–10,12]. Although these approaches may provide insights into the mechanisms associated with narcolepsy, it is important to note that many features of sleep–wake behavior are preserved despite orexin dysregulation.

3. Classic phenomenological models

Early mathematical models of sleep were primarily phenomenological and focused on the nature of the interaction between the sleep and circadian systems. In the two-process model, the timing of human sleep–wake behavior is described by the interaction of circadian (Process C) and homeostatic (Process S) drives, and many features of human sleep–wake behavior have been explained in terms of these interactions [1,68]. Since their original phenomenological postulation, Process C and Process S have been linked to physiological correlates: the molecular and neuronal rhythms in the SCN mediate Process C while the sleep-dependent changes in EEG slow wave activity (SWA; power density in the 0.75–4 Hz band) and extracellular adenosine concentrations are associated with Process S. However, the physiological basis for the interaction of these mechanisms is less clear, though it is likely that this interaction is mediated through the neuronal network governing sleep regulation. The authors of several recent physiologically-based mathematical models have related the dynamics of their models to the two-process model [10,69,70], and we will address this relationship more formally in Section 5.

The Kronauer circadian model, based on a van der Pol oscillator, has also been highly influential in the sleep field [3]. It focused on the functioning of the circadian clock and the implications of this clock function for sleep–wake behavior, and, in particular, it has been applied to questions of optimal scheduling of sleep–wake behavior under many conditions. The van der Pol formalism has been capable of describing several key features of the self-sustaining oscillation of the circadian pacemaker including the ability of the oscillations to be synchronized by external zeitgebers, and the frequency dependence of transitions from constant phase relationships to periodically varying phase relationships. When coupled with another oscillator representing the rest-activity cycle, the interacting oscillators capture both entrained and free-running human sleep–wake behavioral data with appropriate phase relations between core body temperature, a marker of the circadian rhythm, and the timing and duration of sleep [3]. Although there are now models that capture the workings of the intracellular molecular circadian clock [71,72] and the activity of SCN neurons [33], the ability of the Kronauer model (and its variations) to capture these features has led to the use of this model to represent SCN inputs to physiologically-based sleep–wake network models [13,73–75]. In these models, behavioral and neuronal feedbacks to the SCN have been incorporated as light and non-photic inputs to the Kronauer model.

4. Physiological models of sleep–wake regulatory networks

The reciprocal interaction model proposed by McCarley and Hobson may be considered one of the first physiologically-based models of (REM) sleep regulation [5]. Using Lotka–Volterra-type equations, this model focused on understanding the basis of the ultradian cycling between REM and NREM sleep states based on the interactions between cholinergic neurons in the pontine gigantocellular tegmental field and noradrenergic cells in the LC. This model, and the subsequent limit cycle-based refinement [6], introduced a mathematical approach to bridging the conceptual gap between neuronal activity and behavior that is the primary goal of the recent generation of physiological models of sleep–wake regulation. Although the formalisms of the Hobson–McCarley model have been superseded by formalisms arising out of the field of computational neuroscience, the dynamics of this model are preserved in the reciprocal interaction structure present in several recent models as part of their REM sleep regulatory circuitry [7,8,11,14,76–80].

Table 1 summarizes the recent physiological models of sleep–wake regulatory networks considered in this review (distinct models were first introduced in the following references [7–12]). To facilitate comparison, we broadly classify them in terms of

network structure, specifically the conceptual model motivating the REM sleep generating mechanisms in the model, and the mathematical formalism used to represent neuronal population activity. In this section, we describe these classifications, indicate model similarities justifying the classification, and note specific model differences. Modeled behaviors are discussed in Section 6.1.

4.1. Network structures

Comparing network structures among the recent models can be difficult because they include different sleep- and wake-promoting neuronal populations, and the included external inputs, such as the circadian drive, target different populations. However, if we consider the primary neuronal populations promoting the states of wake, NREM sleep and REM sleep included in each model and the effects of direct or indirect projections between them, we can identify basic similarities and differences in network structures. Similarities include the mechanism for transitions between wake and sleep states. Differences stem from the REM-sleep generating mechanisms included in the models. Some models do not separately consider REM sleep; those that do consider REM sleep are based on network structures that reflect either the reciprocal interaction or mutual inhibition hypotheses for REM sleep generation.

All models incorporate mutually inhibitory synaptic interactions between wake-promoting and NREM sleep-promoting populations as proposed in the conceptual model of the sleep–wake flip-flop switch (reviewed in [20], Fig. 2). Wake-promoting populations in the models include the LC, DR, TMN, while the VLPO is the primary NREM sleep-promoting population included in most models. Sleep–wake transitions are promoted by a homeostatic sleep drive based on the somnogenic action of adenosine. Its primary effect is on the activity of the NREM sleep-promoting population such that increasing values promote activation and the transition from wake to sleep (see Section 4.3). The Phillips and Robinson model consists primarily of this sleep–wake flip-flop switch with other external inputs, but it does not include REM sleep generating mechanisms (Fig. 2A). In the other models, the sleep–wake switch is coupled to other populations involved in REM regulation.

The Tamakawa et al., Diniz Behn et al. and Diniz Behn and Booth models all incorporate the reciprocal interaction hypothesis for REM sleep generation in their network structures [7,8,11]. A basic network structure extracted from these models includes the sleep–wake switch with homeostatic sleep drive coupled to a REM sleep-promoting population (Fig. 2B). In all models, the reciprocal interaction hypothesis is reflected in a direct inhibitory projection from the wake population to the REM sleep population and a net excitatory feedback projection from the REM sleep to the wake population. The Tamakawa et al. and Diniz Behn and Booth models additionally include a population that is active during both wake and REM sleep [7,11], which in the Tamakawa et al. model mediates the excitatory feedback projection from the REM sleep to wake population. All models include direct inhibitory projections from the NREM sleep-promoting to the REM sleep population, which is augmented in the Diniz Behn et al. model with a net excitatory projection from an extended VLPO population [8]. The Tamakawa et al. model includes multiple neuronal populations with the same state-promoting properties, but the authors group them into the four primary clusters of populations promoting wake, NREM sleep, REM sleep and wake–REM sleep [7].

The Rempe et al. and Kumar et al. models are based on mutual inhibition hypotheses for REM sleep generation [10,12]. In a basic network structure for these models, the sleep–wake switch with homeostatic sleep drive is coupled to REM-on and REM-off populations with mutual inhibitory projections between them (Fig. 2C). The models differ in the proposed coupling projections. Both models include an inhibitory projection from the wake-promoting population to the REM-on population, while the Kumar et al. model also includes a direct excitatory projection from the wake-promoting population to the REM-off population. Additionally, both models include indirect projections from the NREM-sleep promoting population to the REM-off population: in the Rempe et al. model, the indirect path targets the extended VLPO before reaching the REM-off population while in the Kumar et al. model, an orexinergic population mediates the projection. The Rempe et al. model does not include any feedback projections from the REM regulating populations to the sleep–wake switch. In the Kumar et al. model, an indirect feedback projection from the REM-off population to the wake population is mediated by the orexingeric population.

4.2. Model formalisms

In all models, the output variables of interest are the average firing rates of the state-promoting neuronal populations, as shown in Fig. 1. Behavioral state is then interpreted according to the state-promoting populations that are firing at rates exceeding defined thresholds. The models differ by the type of formalism used to describe population firing rate: one type is based on standard firing rate models for neuronal population activity and the other type modifies equations for the excitable behavior of a single neuron to represent population activity.

Firing rate models typically follow the form developed by Wilson–Cowan [86] in which the average firing rate of population X, f_X (in Hz), depends nonlinearly on the firing rates of presynaptic populations, f_Y (in Hz), and other external inputs to the population, I_j:

$$\tau_X \frac{df_X}{dt} + f_X = S_X\left(\sum_Y g_{YX} f_Y + \sum_j I_j\right), \tag{1}$$

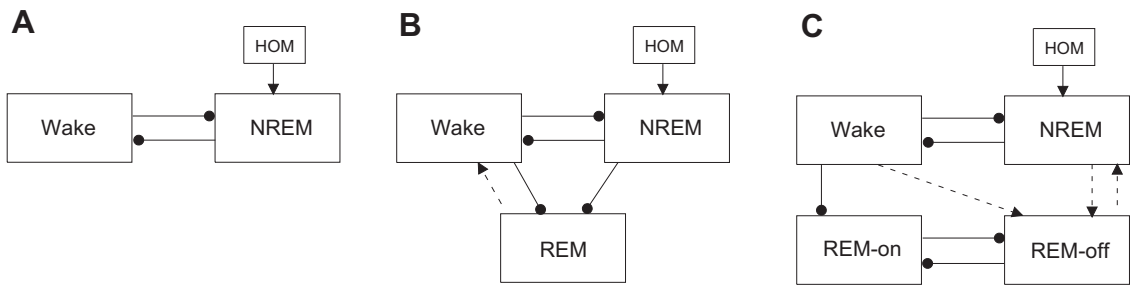

Fig. 2. Schematics of basic network structures shared among the physiologically-based models of sleep–wake regulatory networks. Neuronal populations promoting states of wake, NREM sleep and REM sleep interact through excitatory (arrows) or inhibitory (filled circles) synaptic projections. Solid lines represent direct projections shared among models; dashed lines indicate indirect projections or projections unique to individual models. A: sleep–wake switch network with a homeostatic sleep drive (HOM) modulating state transitions [9]. B,C: basic network structure shared among models based on the reciprocal interaction hypothesis for REM sleep generation (B) [7,8,11] and on the mutual inhibition hypothesis for REM sleep generation (C) [10,12].

where X and Y can be W = wake, S = NREM, R = REM-on and NR = REM-off. Parameters g_{YX} weight the effect of presynaptic firing rate f_Y on population X with the sign (positive or negative) indicating whether synaptic input is excitatory or inhibitory. The firing rate response function S_X is monotonically increasing and usually sigmoidal in shape (Fig. 3A), although other variations have been proposed [87,88]. The time constant τ_X dictates firing rate changes on the population level.

An alternative formulation for the firing rate equation, based on neural mass theory (reviewed in [87]), is employed by the Phillips and Robinson and Tamakawa et al. models. In this form, average firing rate of population X, f_X (in Hz), depends nonlinearly on the mean soma voltage of neurons in the population, V_X, whose level changes depending on firing rates of presynaptic populations, f_Y (in Hz), and external inputs, I_j:

$$\tau_X \frac{dV_X}{dt} + V_X = \sum_Y g_{YX} f_Y + \sum_j I_j, \quad f_X = S_X(V_X). \tag{2}$$

Both of these firing rate formalisms can be derived from equations for the membrane voltage of individual neurons synaptically coupled in the population [88], and steady state or equilibrium solutions for the two forms are equivalent. The difference lies in the assumed dominant time scale of firing rate response: either the synaptic time constant in Eq. (1) or the membrane voltage time constant in Eq. (2) (see [88] for a full discussion).

The Diniz Behn and Booth model implements a modification of the standard firing rate formalism in order to additionally account for the concentration of neurotransmitters that mediate interactions between neuronal populations and are presumed to play a critical role in sleep–wake regulation [89]. In this modification, average firing rate of population X, f_X (in Hz), depends nonlinearly on the extracellular levels of neurotransmitters expressed by presynaptic populations, c_Y, as well as external inputs, I_j:

$$\tau_X \frac{df_X}{dt} + f_X = S_X\left(\sum_Y g_{YX} c_Y + \sum_j I_j\right),$$
$$\sigma_Y \frac{dc_Y}{dt} + c_Y = T_Y(f_Y), \quad T_Y(f) = \tanh\frac{f}{\gamma_Y}. \tag{3}$$

Neurotransmitter expression depends on population firing rate through the monotonically increasing function T_Y, which saturates at 1, a normalized value for maximum expression levels (Fig. 3B). The parameter σ_Y dictates the time scale of neurotransmitter release on the population level and γ_Y governs the sensitivity of release to increases in firing rate. This formalism does not differentiate synaptic and extrasynaptic neurotransmitter concentrations [90]. Rather, in the spirit of a mean field approximation, it represents an approximate spatial and temporal average over these two types of neurotransmission: strictly phasic synaptic neurotransmission in which neurotransmitter concentrations are tightly regulated in the synaptic cleft, and combined phasic and tonic neurotransmission in which neurotransmitter concentrations may spill over and diffuse from the synaptic cleft to activate extrasynaptic receptors. Experimental evidence suggests that the primary neurotransmitters of sleep–wake regulation, noradrenaline, serotonin, GABA and acetylcholine, may all participate in synaptic and extrasynaptic signaling [91–93]. To permit model analysis, a reduced formalism where neurotransmitter release response is instantaneous such that $c_Y(t) = T_Y(f_Y(t))$ has also been considered [79,80]. Modeling time-varying neurotransmitter levels allows for the inclusion of different time scales for firing rate and synaptic dynamics, such as modeling the slow decay or adaptation of synaptic currents. These different time scales can be pertinent in replicating the highly variable and faster transition dynamics that are observed in rodent sleep.

The second type of model formalism, implemented in the Diniz Behn et al., Rempe et al. and Kumar et al. models, uses a simplified

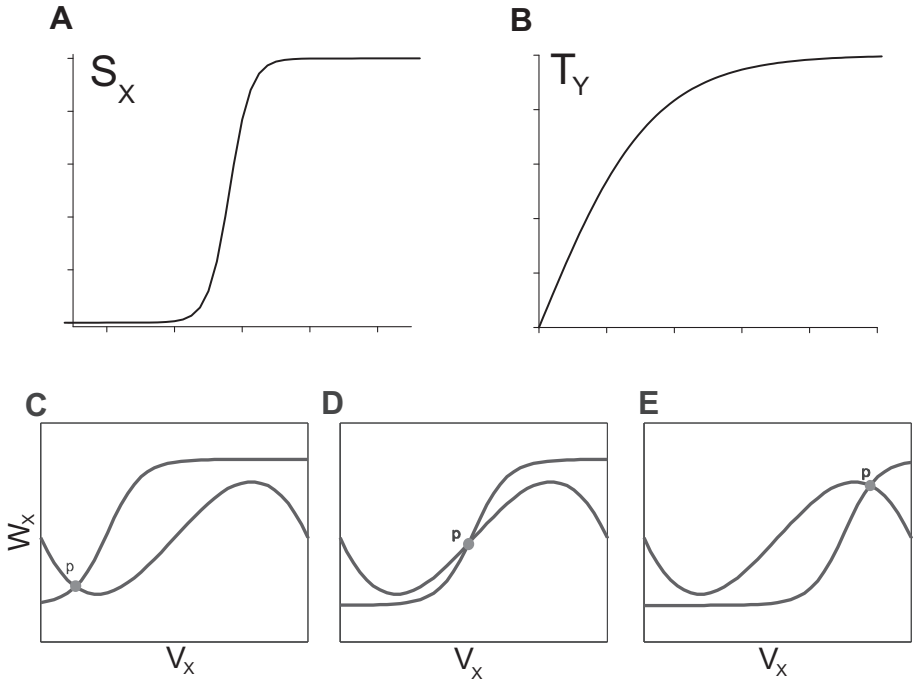

Fig. 3. A: sigmoidal-shaped firing rate response function, S_X, usually used in firing rate model formalisms. B: saturating neurotransmitter expression function, T_Y, used in our firing rate and neurotransmitter model formalism. C–E: nullcline curves for the Morris–Lecar model in the $V_X - W_X$ phase plane. A fixed point p occurs at the intersection of these nullclines. Depending on the level of inputs to a population, the cubic-shaped V_X nullcline and the sigmoidal W_X nullcline intersect on the left branch of the V_X cubic defining a stable fixed point (C), on the middle branch of the V_X cubic defining an unstable fixed point (D) or on the right branch of the V_X cubic defining a stable fixed point (E).

model for the excitable behavior of a single neuron, namely the Morris–Lecar model [94,95], to represent population activity. Specifically, with appropriate scaling of time constants and variable values, the model variable for membrane voltage, V, is interpreted as the average firing rate of a neuronal population, V_X (in Hz) which depends on intrinsic population dynamics, $I_{\text{ion}}(V_X, W_X)$, the firing rates of presynaptic populations, V_Y (in Hz), and external inputs, I_j:

$$\begin{aligned} C\frac{dV_X}{dt} &= I_{\text{ion}}(V_X, W_X) + \sum_Y g_{YX}V_Y + \sum_j I_j, \\ I_{\text{ion}}(V_X, W_X) &= -g_{Ca}\, m_\infty^3(V_X)(V_X - E_{Ca}) \\ &\quad - g_K W_X (V_X - E_K) - g_L(V_X - E_L), \\ \frac{dW_X}{dt} &= \phi \frac{(w_\infty(V_X) - W_X)}{\tau_X(V_X)}. \end{aligned} \tag{4}$$

The variable W_X, which controls gating of a potassium-mediated membrane current, is interpreted as a recovery variable. The steady state gating functions m_∞ and w_∞ are sigmoidal. Synaptic inputs from other populations and external inputs appear as additive terms modulating firing rate response. In using this model formalism, the focus is not on model properties that generate action potential firing as a result of the voltage-dependent membrane ionic currents. Instead, focus is put on the ability of the model to maintain stable steady V_X values or stable oscillating V_X solutions. These solutions are most readily visualized in the $V_X - W_X$ phase plane by the arrangement of the equation nullclines (Fig. 3C–E) [88,95]. The V_X nullcline ($dV_X/dt = 0$) has the typical cubic shape of neuronal membrane models and the W_X nullcline ($dW_X/dt = 0$) is sigmoidal. Intersection points of the nullclines define fixed point or equilibrium solutions. Depending on the net effect of synaptic and other external inputs to the population, a fixed point can exist on the left branch of the cubic V_X nullcline defining a stable state with low firing rate (Fig. 3C) or it can exist on the right branch of the V_X cubic defining a stable high firing rate state (Fig. 3E). For moderate values of synaptic or external inputs, nullclines intersect on the middle branch of the V_X cubic defining an unstable fixed point (Fig. 3D). In this case, the model exhibits stable periodic solutions which represent intrinsic periodic activation of the population.

The firing rate and Morris–Lecar model formalisms are similar in that they support stable solutions in which a population exhibits either a high activity level or a low activity level, and transitions between these states are fast. The most significant difference between the two types of model formalisms is the ability of the Morris–Lecar model to display stable, oscillatory solutions, that represent self-sustaining oscillatory behavior of a single population. None of the firing rate model formalisms possess this ability, so oscillatory behavior in firing rate model networks requires the interaction of multiple populations and/or an external input.

4.3. Homeostatic sleep drive and other network inputs

In the sleep–wake switch component of all models, composed of the mutually inhibitory interactions between the wake- and NREM sleep-promoting populations, transitions in population activity are governed by a homeostatic sleep drive, $H(t)$. This represents a slow accumulated feedback of previous state history on the sleep–wake regulatory system and promotes sleep as a function of prior wakefulness. The model variable H increases during the wake state and decreases during the sleep state with an exponential time course, similar to the two-process model:

$$\frac{dH}{dt} = \begin{cases} \frac{H_{\max} - H}{\tau_W} & \text{in wake} \\ \frac{H_{\min} - H}{\tau_S} & \text{in sleep} \end{cases}. \tag{5}$$

While H is always restricted to be positive, some models include saturating limits, $H_{\max}$ and $H_{\min}$, and different time constants, τ_W and τ_S, for the increase and decrease, respectively, of H. The simulated action of H in all models is on the NREM-sleep promoting population as suggested by the effects of adenosine on the VLPO [64], although the Rempe et al. model additionally includes an action of H on the wake-promoting population [10]. In accordance with the effects of adenosine, H acts on the NREM population such that high levels of H promote its activation, and low H levels permit inactivation. This action of H is modeled as an additive input to the NREM population [7,9,10,12], as an effect on its firing rate response function [11], and by modulating the synaptic inhibition from the wake to the NREM population [8]).

Circadian modulation of sleep–wake behavior is simulated in the models by the inclusion of an external circadian drive representing the signal of the circadian clock propagated throughout the brain by the SCN. The circadian drive has been modeled as a simple 24 h sinusoidal function [9,69,78], as the skewed sinusoidal function derived by the two-process model [10,12] and by circadian oscillator models that take into account the response of the molecular clock to photic and nonphotic inputs [73–75]. The site of action of the circadian drive varies among models reflecting incomplete experimental characterization of the anatomy of the direct and indirect projections between sleep–wake centers and the SCN. Models simulate the circadian drive as targeting only the NREM population [9], distributing effects among multiple sleep- and wake-promoting populations [7,10,78] and acting through orexinergic populations [12]. Physiologically, the molecular circadian clock induces higher neural activity in the SCN during daylight hours and lower activity levels during the night [49]. Assuming that SCN neural activity propagates its circadian signal, models replicating human behavior simulate the action of the circadian drive as inhibiting sleep and/or promoting wakefulness [9,10,12], while models replicating rodent behavior simulate opposite effects [7,78].

Similar formalisms can be used to track other physiologically relevant extracellular variables. For example, as described previously, several of the sleep–wake network models include external inputs from orexinergic neurons [8–10,12] that target the wake-promoting populations and support the waking state.

4.4. Modeling variability in sleep–wake behavior

Sleep–wake architecture is characterized by bouts, or episodes, that are scored as a contiguous state (wake, NREM sleep, or REM sleep). Typically, bouts in experimental data are scored in 10 or 30 s epochs, and this convention has been adopted by mathematical modelers who "score" simulated sleep–wake behavior in order to compare it with experimental data. The minimum bout length is defined by the scoring epoch, and the maximal bout length is determined by the maximal time period of activation of the wake-, NREM sleep-, or REM sleep-promoting populations.

A defining characteristic of rodent sleep–wake behavior is its variability. During the active period, rodents routinely fall into NREM sleep with REM sleep occurring only occasionally. During the rest period, brief wake bouts fragment NREM sleep episodes and REM bouts occur with very little regularity. In humans, while normal sleep–wake behavior displays stereotypical patterning based on average statistics, individual sleep recordings are highly variable with brief wake episodes interrupting NREM sleep and REM–NREM cycle periods showing standard deviations on the order of tens of minutes above the mean 90 min cycle period [96]. As discussed below in Section 6.2, higher order statistical analysis of sleep–wake recordings has suggested that variability in the durations of wake bouts and sleep bouts may, in fact, have a structure that is conserved across rodent and human sleep. For

modeling sleep–wake regulation, then, the addition of noise to a model network may provide additional opportunities for model fitting beyond the basic requirement that the noise does not disrupt the ability to robustly exhibit stereotypical sleep–wake patterning.

In most of the sleep–wake network models, robustness of model dynamics to noise has been investigated by adding stochastic terms to firing rate equations [7–10]. Such additive noise provides variability in state transition dynamics, but investigators did not test whether the higher statistical structure was replicated. In an effort to replicate the variability observed in rodent sleep–wake recordings, the Diniz Behn and Booth models include three key physiological sources of noise [11,14]:

(1) Variability in neurotransmitter release that is correlated with, but not determined by, the firing rate of the presynaptic population;
(2) Variability in the level of the homeostatic sleep drive;
(3) Random excitatory inputs from presynaptic populations that are external to the network represented in the model.

Variability in neurotransmitter release and in the homeostatic sleep drive are motivated by the stochastic nature of synaptic transmission and receptor binding, while random excitatory inputs simulate activity on excitatory afferents from other brain regions targeting sleep–wake regulatory populations. To incorporate variability of neurotransmitter release into the model, each steady state neurotransmitter release function T_Y in Eq. (3) was multiplied by a noise factor whose amplitude randomly varied (with normal distribution and unit mean) at time points determined by a Poisson process (see [11] for additional details). Variability in the level of the homeostatic sleep drive was modeled by replacing the maximum ($H_{\max}$) and minimum ($H_{\min}$) limits for the homeostatic sleep drive, H in Eq. (5), with normally distributed random numbers that changed values at Poisson process-determined time points. Finally, to incorporate random external inputs to a postsynaptic population X, excitatory pulses of random amplitude arriving according to a Poisson process were added to the argument of the steady state firing rate response functions, S_X. As discussed in more detail in Section 6.2, each of these sources of variability contributed to replicating the higher order statistics of rodent sleep–wake behavior [14].

5. Model dynamics and analysis

All of the sleep–wake network models exhibit biologically appropriate state transition behavior including the universally observed state transition sequence of wake to NREM sleep to REM sleep. The models simulating human sleep replicate consolidated periods of wakefulness with regular NREM–REM cycling during sleep [7,10,12], while models for rodent sleep capture their polyphasic sleep patterning [7,8,11]. Each modeling study describes how network structure and model formalism generate these state transitions. The similarities in network structure and dynamics in the model formalisms identified above support our proposal that the models share common underlying dynamics. As discussed in this section, we claim that transition dynamics of the sleep–wake switch can be equivalent in all model formalisms. We propose that the analysis technique of fast–slow decomposition provides a useful framework for analyzing model dynamics of these networks, and we apply this technique to our reciprocal interaction-based network model to understand transition dynamics.

5.1. The sleep–wake switch is a hysteresis loop

In the majority of models, despite differences in model formalisms, transitions between wake and sleep states generated by the mutually inhibitory sleep–wake switch network occur through a hysteresis loop [7–11]. The sleep homeostat H drives model trajectories between states where either the wake or NREM sleep population is active. The mutual inhibition between populations causes the difference in H levels at which sleep–wake and wake–sleep transitions occur, thereby defining the loop. These hysteresis loop dynamics are equivalent to the behavior of the two-process model, as has been shown for the Phillips and Robinson model [69,70] and the Rempe et al. model [10]. As discussed by Phillips and Robinson [69], the equivalent dynamics provide a physiological basis for the phenomenological two-process model.

Mathematically, the hysteresis loop dynamics of the sleep–wake switch can be formally revealed through fast–slow decomposition [79,97]. This technique exploits the different time scales in a model system to reduce the model into a fast subsystem driven by a slowly varying subsystem. For the sleep–wake switch, the slow time scale of the homeostatic sleep drive, relative to the faster transitions in population activity, provides a natural time scale separation. To illustrate this, we consider the sleep–wake switch network (Fig. 2A) modeled in the reduced form of our firing rate and neurotransmitter formalism (Eq. (3)) under modulation of a homeostatic sleep drive H:

$$\begin{aligned}
&\tau_W \frac{df_W}{dt} + f_W = S_W(g_{SW}c_S), \quad c_W = T_W(f_W),\\
&S_W(c) = \frac{W_{\max}}{2}\left(1+\tanh\left(\frac{c-\beta_W}{\alpha_W}\right)\right),\\
&\tau_S \frac{df_S}{dt} + f_S = S_S(g_{WS}c_W, H), \quad c_S = T_S(f_S),\\
&S_S(c,H) = \frac{S_{\max}}{2}\left(1+\tanh\left(\frac{c-\beta_S(H)}{\alpha_S}\right)\right),
\end{aligned} \tag{6}$$

where time is in seconds. The sleep homeostat H is governed by Eq. (5) with τ_W = 600 s, τ_W = 700 s, $H_{\max}$ = 1.4 and $H_{\min}$ = −1.6. H affects activation of the NREM population by modulating its half-activation level as $\beta_S(H)$=−1.5H. The steady state neurotransmitter expression functions T_W and T_S are as in Eq. (3) with γ_W = 5 Hz and γ_S = 4 Hz. Waking behavior is defined by $f_W > \theta_W$ = 1.5 Hz. The remaining parameters are: g_{SW} = −2, g_{WS} = −2, $W_{\max}$ = 6.5 Hz, β_W = −0.3, α_W = 0.5, $S_{\max}$ = 5 Hz and α_S = 0.25. Numerical solutions of this network display regular alternations of high f_W activity corresponding to the waking state and high f_S activity corresponding to the sleep state (Fig. 4A) with fast transitions between states.

Fast–slow decomposition takes advantage of the much slower time scales for H activity (600 and 700 s) relative to f_W and f_S activity (5 and 1 s) to decompose this model into a fast subsystem consisting of the equations for f_W and f_S (Eq. (6)) and a slow subsystem consisting of the equation for H (Eq. (5)). As we have shown previously, this decomposition can be done formally by scaling the time constants for H by a small parameter ε, and taking the limit as ε approaches zero [79,80]. Model dynamics are then analyzed in terms of the fast subsystem with the slow variable H considered as a parameter, with values in the interval $[H_{\min}, H_{\max}]$. Computing the bifurcation diagram of the fast subsystem, with respect to H as the bifurcation parameter, reveals a Z-shaped curve of fixed point solutions for f_W (Fig. 4B). For low and high values of H, single stable fixed points exist: high f_W values correspond to the wake state, and low f_W values correspond to the sleep state. For an interval of H values, the high and low stable branches of the bifurcation curve overlap, separated by a branch of unstable fixed points, creating a region of bistability. Saddle-node bifurcations form the endpoints of this region and define the transition points between wake and sleep. By choosing θ_W, the f_W threshold defining the wake state and the direction of H evolution, between the stable upper and lower branches of the Z-shaped bifurcation curve, the slow H dynamics drive the trajectory of the full model system around this

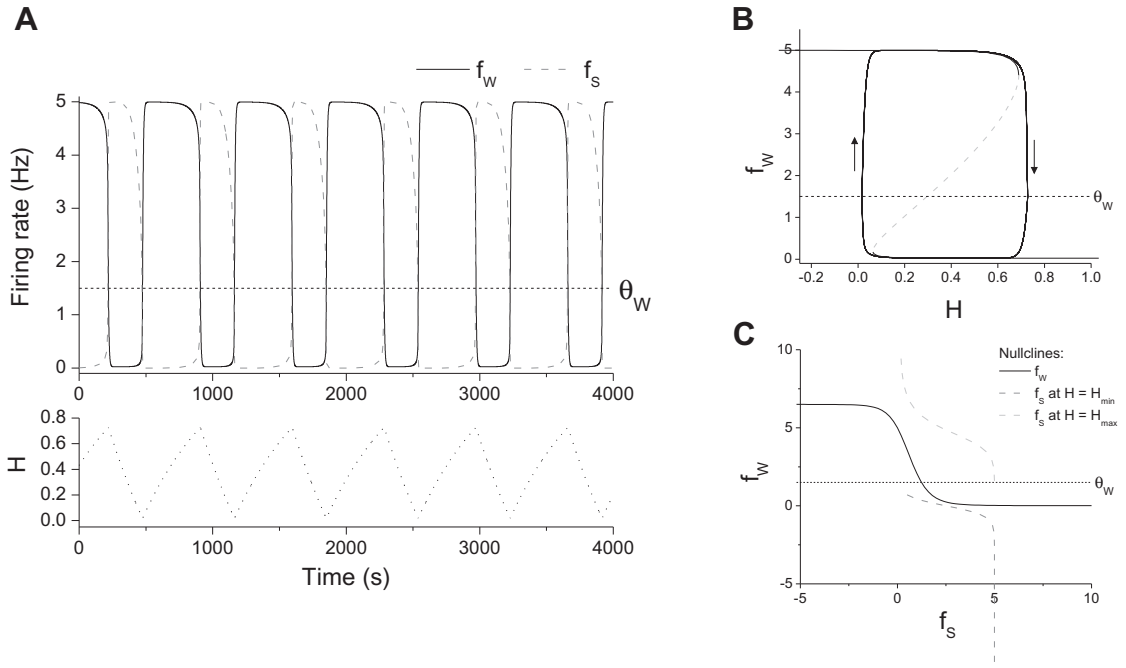

Fig. 4. Fast–slow decomposition of the sleep–wake switch network. A: numerical solutions of the sleep–wake switch network modeled in the reduced form of our firing rate and neurotransmitter model formalism showing regular alternations of wake and sleep states as firing rates of the wake- and sleep-promoting populations, f_W (top trace, solid curve) and f_S (top trace, dashed curve), respectively, alternate between high and low levels. Wake is defined when f_W is above the threshold θ_W (dotted horizontal line). Transitions are governed by the homeostatic sleep drive H (bottom trace, dotted curve) which increases during wake and decreases during sleep. B: bifurcation diagram of the fast subsystem (Eq. (6)) with respect to the homeostatic sleep drive H as a parameter showing the Z-shaped curve of fixed point solutions with stable high f_W and low f_W fixed points (thick solid portions of curve) separated by unstable fixed points (dashed portion of curve). Thin curve shows trajectory of full model traveling clockwise about the hysteresis loop defined by the Z-shaped bifurcation curve (H increases for $f_W \geqslant \theta_W$, H decreases for $f_W < \theta_W$). C: nullcline curves of the fast subsystem (Eq. (6)) in the $f_S - f_W$ phase plane. The f_S nullcline (dashed curves) is discontinuous reflecting the discontinuity of the H nullsurface (Eq. (5)) with values of $H = H_{\max}$ if $f_W \geqslant \theta_W$ and $H = H_{\min}$ if $f_W < \theta_W$.

region of bistability to produce stable, periodic oscillations consisting of alternating periods of high f_W and high f_S activity.

Inputs to either population affect the H values of the saddle-node bifurcations, or knees of the Z-shaped bifurcation curve, to change the timing of state transitions. For example, an oscillating circadian drive targeting the sleep population can rhythmically shift the H values of the knees, which acts similarly to the circadian modulation of the lower and upper thresholds for state transitions in the two-process model.

In an analysis of the existence of hysteresis loop cycling in an equivalent network [80], we identified two general mechanisms by which hysteresis-loop cycling is lost: the trajectory may approach a stable fixed point of the full model or the H dynamics may trap the trajectory near the threshold value $f_W = \theta_W$. In terms of the fast subsystem bifurcation diagram (Fig. 4B), these mechanisms can be understood as follows:

(1) If a stable branch of the Z-shaped bifurcation curve intersects the line $H = H_{\min}$ below the threshold $f_W = \theta_W$ or intersects the line $H = H_{\max}$ above the threshold $f_W = \theta_W$, the intersection point will be a stable fixed point of the full model. Regardless of initial conditions, the model trajectory will eventually approach the steady state values associated with this stable fixed point;
(2) If a stable branch of the Z-shaped bifurcation curve intersects the threshold, $f_W = \theta_W$, the system will enter into a low-amplitude oscillation about this point.

Inputs to the wake and sleep-promoting populations, either external or synaptic from other populations included in the network, can distort the bifurcation curve of the fast subsystem so that either of these mechanisms destroys hysteresis loop cycling.

A condition for the existence of hysteresis loop cycling suggested by 1), namely the absence of a stable fixed point of the full model, can be graphically defined in the phase plane of the 2-D fast subsystem (Fig. 4C). To illustrate this, we consider the nullcline surfaces of the full model (setting time derivatives to 0 in Eqs. (5) and (6)). The H nullsurface consists of two pieces: $H = H_{\max}$ if $f_W \geqslant \theta_W$ and $H = H_{\min}$ if $f_W < \theta_W$. This defines a discontinuity in the f_S nullsurface at $f_W = \theta_W$. Since there is no explicit H dependence in the f_W equation, the f_W nullsurface is continuous. In the (f_W, f_S) phase plane, an intersection point of the piecewise f_S nullcline with the f_W nullcline corresponds to a fixed point of the full model. However, due to the discontinuity of the f_S nullcline, it may not intersect the f_W nullcline, as shown in Fig. 4C, thus allowing for the existence of hysteresis-loop cycling.

As discussed in more detail in Section 5.3, the higher complexity of the Morris–Lecar model formalism introduces additional dynamics to model solutions so that the sleep–wake flip-flop switch may not exhibit equivalent hysteresis loop dynamics. However, in the Rempe et al. and the Diniz Behn et al. models, parameters are set so that sleep–wake switch dynamics are similar to those generated by a hysteresis loop [8,10]. We can see this similarity by considering model solutions in the phase planes of each population, as described in [8,10]. In particular, activation of either the wake or NREM population corresponds to the existence of a stable fixed point on the right branch of the V_W or V_S cubic nullclines, respectively (as in Fig. 3E). The homeostatic sleep drive acts to shift these cubic nullclines such that state transitions occur when the stable fixed point disappears in a saddle-node bifurcation. These saddle-node bifurcations are thus defined for specific values of the sleep homeostat H, similar to the saddle-node bifurcations in the fast subsystem bifurcation diagrams underlying hysteresis loop dynamics in the firing rate formalism models. Below

we discuss how the Kumar et al. model takes advantage of the additional dynamics of the Morris–Lecar model to induce transitions in the sleep–wake switch in a different manner.

5.2. Dynamics of REM–NREM reciprocal interaction hypothesis networks

We can intuitively understand the dynamics of network models based on the reciprocal interaction hypothesis for REM sleep generation (Fig. 2B) by recognizing that transitions between sleep and wake states generated by the sleep–wake switch occur through hysteresis loop dynamics as described above. Since the classic reciprocal interaction model generates REM–NREM cycling through limit cycle dynamics, we can further expect that during the sleep state, the REM population can repetitively activate as a result of limit cycle dynamics arising through its coupling to the wake-promoting population. Thus, we may expect the dynamics of the sleep–wake network models with reciprocal interaction mechanisms to be governed by a coupled hysteresis loop and limit cycle. To formally reveal and understand these dynamics, we applied fast–slow decomposition to the Diniz Behn and Booth reciprocal interaction-based network modeled in the reduced form of the firing rate and neurotransmitter formalism (Eq. (3)) [79]. This model consists of firing rate equations for the 3 state-promoting populations under the modulation of the homeostatic sleep drive H (Eq. (5)) that affects the activation of the NREM population as in Eq. (6):

$$\begin{aligned}
&\tau_W \frac{df_W}{dt} + f_W = S_W(g_{SW}c_S + g_{RW}c_R), \quad c_W = T_W(f_W),\\
&\tau_S \frac{df_S}{dt} + f_S = S_S(g_{WS}c_W, H), \quad c_S = T_S(f_S),\\
&\tau_R \frac{df_R}{dt} + f_R = S_R(g_{WR}c_W + g_{SR}c_S), \quad c_R = T_R(f_R),
\end{aligned} \tag{7}$$

where steady state firing rate response functions, S_X, and neurotransmitter expression functions, T_X, are defined as in Eqs. (6) and (3), respectively (see [79] for full equations and parameter values). Applying fast–slow decomposition motivated by the slow dynamics of the homeostatic sleep drive defines a three-dimensional fast subsystem (Eqs. (7)) in which H is a parameter. The bifurcation diagrams of the fast subsystem in terms of the bifurcation parameter H are necessarily more complex than in the sleep–wake switch, but an underlying hysteresis loop is still apparent (Fig. 5A and B). For certain parameter values, the f_W bifurcation curve has a general Z-shape, with a branch of stable fixed point solutions that exists for low values of H as in the sleep–wake switch (Fig. 5A). However, the branch of stable solutions that exists for high H values instead consists of stable periodic solutions. Thus, the hysteresis loop is defined by a region of bistability between a branch of stable fixed point solutions representing the wake state, and a branch of stable periodic solutions governing REM–NREM transitions during sleep. In the f_W bifurcation plot, these periodic solutions are of low amplitude and represent small increases in wake population activity as a result of REM population activation. The f_R bifurcation plot reveals high amplitude, stable periodic solutions in f_R that exist for high H values (Fig. 5B). The region of bistability is less apparent in the f_R bifurcation plot since the branch of stable fixed point solutions at low f_R values, corresponding to the wake state, is at the same f_R values as the minimum of the stable periodic solutions (superimposed in the figure). In the full model, then, the slow dynamics of H drive the hysteresis loop dynamics between a state with high f_W and low f_S and f_R activity, representing the wake state, and a state with high f_S activity and alternating high f_R activity with small f_W fluctuations, representing NREM–REM cycling during the sleep state (Fig. 5C).

Model analysis identified that REM sleep dynamics were dependent on the coupling between the sleep–wake switch and the REM population [79]. To explore this dependency we modified the half-activation of the steady state firing rate response function for the REM population, S_R. For high values of this parameter, β_R, the REM population did not activate during the sleep state and model dynamics were completely described by the sleep–wake hysteresis loop. At lower values of this parameter, the REM population activated only prior to the transition from sleep to wake, generating the stereotypical sleep pattern of wake–NREM–REM–wake observed in rodents. For even lower β_R values, the periodic solutions representing NREM–REM cycling appeared in the fast subsystem bifurcation plot, and the fraction of the bistability region over which these periodic solutions existed increased as β_R was further decreased. The bifurcation plots in Fig. 5A and B illustrate the case for the lower values in this range. Thus, by varying a single parameter, REM dynamics could be altered to generate sleep patterns reflective of different species and different circadian phases.

5.3. Dynamics of REM–NREM mutual inhibition hypothesis networks

Both of the model networks based on the mutual inhibition hypothesis for REM sleep generation, the Rempe et al. and Kumar et al. models, employ the Morris–Lecar model formalism whose additional complexity allows different network dynamics. For example, while both models contain a sleep–wake switch under homeostatic modulation to govern transitions between wake and sleep states, the transition dynamics may not necessarily be equivalent to a hysteresis loop. As described above, parameter values are set in the Rempe et al. model so that sleep–wake switch dynamics are similar to a hysteresis loop in which transitions are governed by the homeostatic sleep drive [10]. However, since populations possess the potential for intrinsic oscillatory behavior in this model formalism, the sleep–wake switch need not rely on the sleep homeostat to drive state transitions. Specifically, in the Kumar et al. model, activation of the wake population is associated with a stable fixed point on the right branch of the V_W cubic. Thus, transitions from wake to sleep depend on the homeostatic sleep drive activating the NREM population, causing this fixed point to disappear at a saddle-node bifurcation. Activation of the NREM population, however, may result in unstable fixed points on the middle branch of the V_S cubic nullcline. As a consequence, there is no stable fixed point with high V_S values that attracts the trajectory and, instead, the V_S trajectory may transiently activate, supported by the action potential generating mechanisms of the Morris–Lecar model. In this case, the transition from sleep back to wake, and thus sleep bout durations, are not determined by the sleep homeostat but rather by the intrinsic properties of the NREM population. Rempe et al. exploit this alternate mechanism for generating transitions in the sleep–wake switch in their simulations of narcoleptic sleep behavior. In those simulations, modulation of the influence of an orexinergic population enabled the change in dynamics.

Despite structural similarities to the sleep–wake switch in both mutual inhibition hypothesis models, transitions in the REM-on/REM-off switch are not generated by a hysteresis loop. Instead, both models exploit the intrinsic oscillatory dynamics of individual populations to drive REM–NREM transitions during sleep. In the Rempe et al. model, during the sleep state, the REM-off population is in a regime where nullcline intersections correspond to unstable fixed points and the population intrinsically oscillates. It thus provides alternating episodes of inhibition to the REM-on population allowing it to oscillate with an anti-phase relationship. In the Kumar et al. model, the REM-on population is in the intrinsically oscillating regime during the sleep state, and its alternating inhibition to the REM-off population drives the anti-phase oscillations of the two populations.

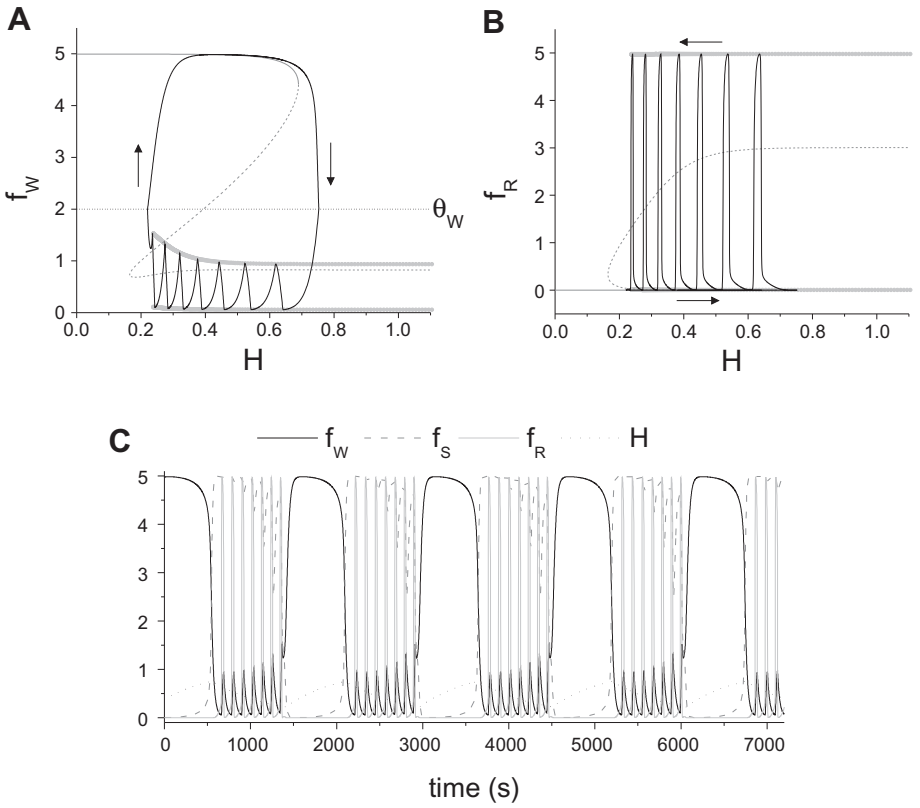

Fig. 5. Fast–slow decomposition of the reciprocal interaction hypothesis network. A,B: bifurcation diagrams of the 3-D fast subsystem (Eq. (7)), with respect to the homeostatic sleep drive H as a parameter, in terms of f_W (A) and f_R (B). Fast subsystem stable solutions consist of a steady high f_W, low f_R state (thick solid curve) representing wake and a periodic solution in which f_R displays high amplitude oscillations and f_W displays low amplitude fluctuation (gray dots). These stable solutions are separated by unstable steady solutions (thin dashed curves). In the full model, the slowly varying sleep homeostat H drives the trajectory (thin solid curve) between these states with H increasing for $f_W \geqslant \theta_W$ and H decreasing for $f_W < \theta_W$. C: time trace of full model trajectory showing alternations in population firing rates between the simulated wake state (high f_W, low f_S, low f_R, H increasing) and NREM/REM cycling during sleep (high f_S, large amplitude f_R oscillations, low amplitude f_W fluctuations, H decreasing). Adapted from [79].

6. Model validation

To bridge the gap between sleep–wake behavior and the neuronal mechanisms underlying its regulation, the output of the recent physiological network models is simulated sleep–wake behavior. Model validation then relies on the replication of behavioral state transitions observed in experimental sleep–wake recordings, accounting for both qualitative and quantitative characteristics. Qualitative features include patterns of state transitions such as the stereotypical transition pattern of wake-to-NREM-to-REM sleep which is observed in all normal mammalian sleep, regular REM–NREM cycling that occurs in human sleep, and appropriate phase relationships between the circadian and sleep–wake cycles. Quantitative measures of sleep–wake behavior have traditionally consisted of basic summary statistics such as time spent in each state and the number and duration of bouts. In many cases, perturbations to normal sleep–wake behavior have been used to provide additional constraints. These perturbations may simulate naturally-occurring pathologies, such as the fragmented sleep–wake behavior that occurs in the sleep disorder narcolepsy, or they may reflect external manipulations such as microinjection of neurotransmitter agonists/antagonists or pharmacological agents. In Section 6.1 we describe some of the diverse aspects of sleep–wake behavior that have been used in the validations of physiologically-based mathematical models.

Although behavioral diversity provides some clear constraints for models, given the complexity of the physiological network models, these measures may still fail to provide sufficient constraints to identify and differentiate proposed model structures and model formalisms. For example, the different network structures of the Rempe et al. and Kumar et al. mutual inhibition-based networks could each account for stereotypical normal human sleep behavior and its disruption by removal of orexinergic inputs as occurs in narcolepsy. The polyphasic nature of rodent sleep may provide richer state transition dynamics to constrain these complex models. The larger number of bouts occurring in rodent sleep facilitates the application of higher order statistical approaches such as survival-based analysis of wake and sleep bout durations; these techniques have been applied to analyze human data as well [98–100], but, to our knowledge, they have not been used to constrain models of human sleep. In Section 6.2, we discuss results illustrating an approach in which features of survival analysis applied to rodent sleep were used to constrain the Diniz Behn and Booth model.

6.1. Reproducing diverse aspects of sleep–wake behavior

Mathematical modeling of sleep–wake behavior has been motivated by experimental observations in a range of species under different conditions. In many cases, these observations have yielded variations of baseline sleep–wake behavior that could be used to constrain a physiologically-based model; some of these modeled behaviors are summarized in the last column of Table 1. In human sleep, baseline sleep–wake behavior, with its strong circadian modulation, often provides the initial assessment of model solutions [7,76]. Further constraints on these models arise from specific disease phenotypes, such as narcolepsy [10,11], or externally-imposed perturbations to baseline human sleep–wake behavior

caused by sleep deprivation [8,82,10,11], internal desynchrony [72,12], or caffeine administration [80].

In models of rodent sleep–wake behavior, similar perturbations including circadian modulation [76] and orexin dysregulation (resulting in a narcolepsy-like phenotype) [75] have been used to constrain models. The differences in sleep–wake behavior across species, produced by a putatively conserved network of neurons, have also been used as constraints [6,81,101]. In addition, modeling rodent behavior allows us to take advantage of data from more invasive experiments that can only be done in animal models. Numerous experimental studies have investigated the role of specific neuronal populations and neurotransmitter interactions in the regulation of sleep–wake states through targeted microinjection of neurotransmitters, their agonists or antagonists in the behaving animal [23,102,103]. For example, in the rat, Mallick et al. [23] investigated the role of the LC in REM sleep regulation by microinjecting GABA and ACh agonists and antagonists into the LC and monitoring REM sleep behavior for the subsequent 4 h. Such experiments directly manipulate components of proposed sleep–wake regulatory networks and assess the effects on sleep behavior, thereby providing significant constraints on model network structure and dynamics. Simulations of such experiments were performed using the Tamakawa et al. model where the action of injected agents was simulated by adding fixed external inputs to specific populations [7]. We refined these simulations in the firing rate and neurotransmitter model formalism: the explicit tracking of neurotransmitter concentrations in this formalism allows for more realistic simulation of the effects of injected neurotransmitters, their agonists or antagonists [11].

In addition to providing novel constraints for the model, the comparison of simulated results to agonist/antagonist experiments can provide valuable insights into the mechanisms underlying experimental observations. As an example, in the Mallick study, some pairs of neurotransmitter agonists/antagonists exerted opposite effects on certain sleep–wake states [23], but trends were not as clear for all pairs or all states. This type of result, though difficult to interpret, is not unexpected given the different actions of agonists and antagonists. Namely, agonists act on the network during all sleep–wake states, so every state and state transition may be affected by their presence. In contrast, antagonists exert an effect only when the relevant neurotransmitter is present. Because the presence of specific neurotransmitters in sleep–wake centers is state dependent, this implies that antagonists directly affect only a subset of states and state transitions.

In addition to targeted microinjection, recently developed experimental techniques such as optogenetic stimulation offer new methods to probe the role of specific neural populations and their interactions in the control of sleep–wake behavior [104–106]. Given the challenges of interpreting resulting changes in sleep behavior of such experiments in terms of conceptual models of sleep–wake regulatory networks, we propose that physiologically-based models can play an important role during the entire experimental process. They can serve as a test bed for proposed experiments to determine which manipulations would result in significant and observable effects on sleep behavior. Results of simulated experiments and analysis of model dynamics can provide a framework for interpreting experimental results. Additionally, different model network structures and model formalisms can be tested to account for discrepancies between experimental and model results.

6.2. Survival analysis of bout durations

Recently, survival analysis of state bout durations has been applied as a higher-order metric for sleep–wake behavior that can quantitatively distinguish experimental conditions and disease states. Early studies using survival analysis identified key qualitative differences in the distributions of wake and sleep bout durations. Namely, wake bout durations displayed power-law distributions (proportional to $t^{-\alpha}$) while sleep bout durations exhibited exponential distributions (proportional to $e^{-\beta t}$) [107]. Interestingly, these distribution profiles persisted across species [108], though they exhibited alterations in the presence of different conditions such as disease or genetic mutation [77,98–100,109]. Although recent work has questioned whether wake distributions are best characterized by a strict power-law distribution or a multi-exponential distribution [110], the key point of this analysis is the identification of distinct, qualitative differences between wake and sleep bout distributions.

Replicating distributions of bout durations that necessarily reflect highly variable state transition dynamics is a challenge for the physiological sleep–wake network models whose dynamics are governed by an underlying deterministic system. Using the Diniz Behn and Booth model, we investigated whether it could generate rodent sleep–wake behavior that matched summary statistics of experimentally recorded behavior as well as wake and sleep bout distributions that followed power-law-like and exponential profiles, respectively [14]. To induce state transition variability, the three physiological sources of variability described in Section 4.4 were included: (1) variability in neurotransmitter release, (2) variability in the level of the homeostatic sleep drive, and (3) external random excitatory inputs to the wake-, REM sleep- and wake/REM sleep-promoting populations.

The model generated realistic rat sleep–wake patterning with standard summary statistics not differing significantly from those reported for experimental rat sleep recordings in the light period (two-sample t-test, $p < 0.05$, [111]). More importantly, distribution profiles of simulated wake and sleep (NREM and REM sleep states combined) bout durations qualitatively exhibited the appropriate profiles (Fig. 6). Wake bout durations between 10 and 480 s followed a power-law distribution (Fig. 6A), while sleep bout durations followed an exponential distribution (Fig. 6B). Fitting either distribution with alternate functions, such as an exponential function for the wake durations or a power-law function for sleep durations, resulted in larger least-squared errors and lower r^2 values.

Obtaining the appropriate distribution profiles of wake and sleep bout durations most certainly depended on the noise sources included in the model. However, network structure also played a significant role, especially in replicating the power-law-like profile of wake bout durations. Model analysis showed that, in the deterministic model with all noise sources removed, wake bout durations displayed a bimodal profile reflecting two network mechanisms for wake bout generation: homeostatically governed wake bouts with longer durations and shorter wake bouts associated with the termination of REM bouts as a result of the reciprocal interaction mechanism for REM sleep. Variability in neurotransmitter and homeostatic sleep drive levels introduced more variance to this bimodal distribution. However, in order to achieve the power-law-like profile of wake bouts, the brief wake bouts initiated by external excitatory inputs were required to have shorter average duration than the brief post-REM wake bouts. Thus, the existence of three separate mechanisms with distinct time constants to generate wake bouts along with the appropriate coordination of these mechanisms were key in producing a power-law-like profile of wake bout durations. Interestingly, these results are more consistent with a multi-exponential distribution for wake bout durations rather than a strict power law distribution.

An exponential distribution for sleep bout durations was less sensitive to specifics of network structure since it can be generated by random interruptions of the sleep state. We found that the longest duration sleep bouts (>200 s) followed approximately exponential distributions for every combination of stochastic

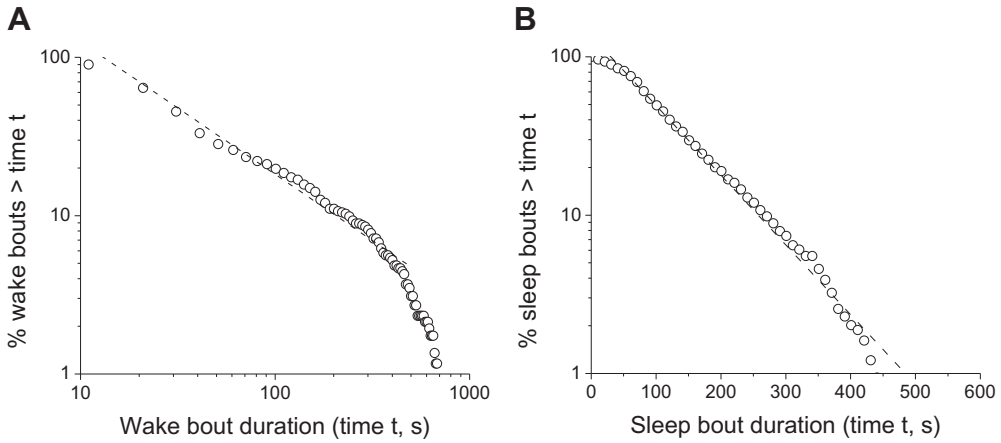

Fig. 6. Survival plots of wake bout (A) and sleep bout (B, NREM and REM sleep states combined) durations exhibiting power law-like and exponential distributions, respectively, computed from simulated rodent sleep using our reciprocal interaction hypothesis sleep–wake regulatory network model with physiologically motivated sources of variability. Dashed lines show optimal fits to power law (A: $10^{(2.935)}t^{(-0.837)}$, $r^2 = 0.9724$) and exponential (B: $10^{(2.133)}\exp^{(-0.0101t)}$, $r^2 = 0.9882$) functions. Adapted from [14].

elements included in the model. Obtaining an initial exponential profile for shorter sleep bouts depended on the presence of random excitatory inputs to the wake-promoting populations that introduced higher fragmentation of the NREM state.

While the use of survival analysis to characterize experimentally recorded sleep–wake behavior is relatively new and has been applied in only a limited number of studies, it provides significantly tighter constraints on results of sleep–wake network models than standard summary statistics. Further work is clearly needed to make this analysis standard for sleep–wake regulation modeling. For example, the effect of different forms of variability included in model networks on bout duration distributions should be analyzed, and the ability of this analysis to distinguish different network structures or different model formalisms needs to be investigated. This approach also provides an excellent opportunity to evaluate the interactions of deterministic and stochastic components and assess their contributions to overall model dynamics.

7. Conclusions

The influence of the phenomenological two-process model, coupled oscillator models and the reciprocal interaction model on our scientific progress in understanding sleep and circadian rhythms cannot be overstated. However, the recent advances in clarifying the neural anatomy and physiology involved in the regulation of sleep and circadian rhythms require more detailed and physiologically-based mathematical models. Indeed, mathematical models have the greatest impact when modeled mechanisms can be directly correlated with physiological mechanisms and model outputs with observed measurements. In the recent physiologically-based mathematical models of sleep–wake regulatory networks, existing experimental results are incorporated and model predictions include specific, testable hypotheses. Thus, these models have the potential to contribute much to current experimental investigations of sleep and circadian rhythms. However, these models are very complex, reflecting both intricate network structures and the highly nonlinear dynamics inherent in the mathematical formalisms used. In this review we identified common features among these models including network structures, model dynamics and approaches for model validation. Our hope is that identifying these commonalities will help to propel understanding of both the mathematical models and their underlying conceptual networks, and focus directions for future experimental and theoretical work.

In closing, we would like to comment on what we see as the current challenges facing mathematical modeling of sleep–wake and circadian regulation. Although the field of computational neuroscience is sufficiently broad and mature to provide appropriate mathematical formalisms to model brain activity at many temporal and spatial scales, detailed simulation of sleep–wake behavior requires the appropriate integration of formalisms into multi-scale models. The models reviewed here reflect current formalisms for modeling neural activity at the population level and synaptic interactions among neuronal populations. However, many of these formalisms were developed to describe the behavior of cortical networks. The brainstem and hypothalamic populations involved in sleep–wake regulation and the complexity of their neuronal signaling, particularly when neuropeptides are involved, may require new formalisms. Similarly, the next generation of circadian models requires new approaches to integrate models of the molecular clock with models of SCN neurons and to appropriately incorporate the effects of photic and non-photic inputs on this system. Just as the dynamics of the two-process model can be interpreted in terms of recent physiological sleep–wake models, future physiologically-based circadian models may provide a context for the dynamics of the Kronauer circadian model based on the van der Pol oscillator.

Another major challenge is model validation. Reliance on the replication of qualitative features of behavioral state transitions, which was sufficient for the phenomenological models, does not provide sufficient constraints on highly complex models. The increasing use of higher order statistical measures to characterize experimental sleep–wake recordings, particularly in humans [100], is an important advance which modeling studies can adopt to improve model validation. As newer experimental techniques for recording and stimulating neural activity are applied to understand sleep and circadian rhythms in behaving animals [105], these data can offer novel constraints for models. Furthermore, advanced techniques that more closely incorporate experimental data and mathematical models [112,113], such as data assimilation that is extensively used in weather prediction modeling, offer sophisticated methods for model constraint and can strengthen the role of mathematical modeling in the scientific investigation of sleep–wake behavior.

Acknowledgment

This material is based upon work supported by the National Science Foundation under Grant No. DMS-1121361.

References

[1] A.A. Borbely, A two process model of sleep regulation, Hum. Neurobiol. 1 (1982) 195.
[2] S. Daan, D.G. Beersma, A.A. Borbely, Timing of human sleep: recovery process gated by a circadian pacemaker, Am. J. Physiol. 246 (1984) R161.
[3] R.E. Kronauer, C.A. Czeisler, S.F. Pilato, M.C. Moore-Ede, E.D. Weitzman, Mathematical model of the human circadian system with two interacting oscillators, Am. J. Physiol. 242 (1982) R3.
[4] S.H. Strogatz, Human sleep and circadian rhythms: a simple model based on two coupled oscillators, J. Math. Biol. 25 (1987) 327.
[5] R.W. McCarley, J.A. Hobson, Neuronal excitability modulation over the sleep cycle: a structural and mathematical model, Science 189 (1975) 58.
[6] R.W. McCarley, S.G. Massaquoi, A limit cycle mathematical model of the REM sleep oscillator system, Am. J. Physiol. 251 (1986) R1011.
[7] Y. Tamakawa, A. Karashima, Y. Koyama, N. Katayama, M. Nakao, A quartet neural system model orchestrating sleep and wakefulness mechanisms, J. Neurophysiol. 95 (2006) 2055.
[8] C.G. Diniz Behn, E.N. Brown, T.E. Scammell, N.J. Kopell, A mathematical model of network dynamics governing mouse sleep–wake behavior, J. Neurophysiol. 97 (2007) 3828.
[9] A.J. Phillips, P.A. Robinson, A quantitative model of sleep–wake dynamics based on the physiology of the brainstem ascending arousal system, J. Biol. Rhythms 22 (2007) 167.
[10] M.J. Rempe, J. Best, D. Terman, A mathematical model of the sleep/wake cycle, J. Math. Biol. 60 (2010) 615.
[11] C. Diniz Behn, V. Booth, Simulating microinjection experiments in a novel model of the rat sleep–wake regulatory network, J. Neurophysiol. 103 (2010) 1937.
[12] R. Kumar, A. Bose, B.N. Mallick, A mathematical model towards understanding the mechanism of neuronal regulation of wake–NREMS–REMS states, PLoS ONE 7 (2012) e42059.
[13] R. Gleit, C.G. Diniz Behn, V. Booth, Modeling inter-individual differences in spontaneous internal desynchrony patterns, J. Biol. Rhythms 28 (2013) 339.
[14] C.G. Diniz Behn, V. Booth, Modeling the temporal architecture of rat sleep–wake behavior, 2011 Annu. Int. Conf. IEEE Eng. Med. Biol. Soc. (EMBC) (2011) 4713–4716.
[15] V.V. Vyazovskiy, U. Olcese, E.C. Hanlon, Y. Nir, C. Cirelli, et al., Local sleep in awake rats, Nature 472 (2011) 443.
[16] J.M. Krueger, G. Tononi, Local use-dependent sleep; synthesis of the new paradigm, Curr. Top. Med. Chem. 11 (2011) 2490.
[17] M.T. Bianchi, N.A. Eiseman, S.S. Cash, J. Mietus, C.K. Peng, et al., Probabilistic sleep architecture models in patients with and without sleep apnea, J. Sleep. Res. 21 (2012) 330.
[18] A.J. Phillips, P.A. Robinson, E.B. Klerman, Arousal state feedback as a potential physiological generator of the ultradian REM/NREM sleep cycle, J. Theor. Biol. 319 (2013) 75.
[19] C.B. Saper, G. Cano, T.E. Scammell, Homeostatic, circadian, and emotional regulation of sleep, J. Comp. Neurol. 493 (2005) 92.
[20] C.B. Saper, T.C. Chou, T.E. Scammell, The sleep switch: hypothalamic control of sleep and wakefulness, Trends. Neurosci. 24 (2001) 726.
[21] J.A. Hobson, R.W. McCarley, P.W. Wyzinski, Sleep cycle oscillation: reciprocal discharge by two brainstem neuronal groups, Science 189 (1975) 55.
[22] S. Datta, R.R. Maclean, Neurobiological mechanisms for the regulation of mammalian sleep–wake behavior: reinterpretation of historical evidence and inclusion of contemporary cellular and molecular evidence, Neurosci. Biobehav. Rev. 31 (2007) 775.
[23] B.N. Mallick, S. Kaur, R.N. Saxena, Interactions between cholinergic and GABAergic neurotransmitters in and around the locus coeruleus for the induction and maintenance of rapid eye movement sleep in rats, Neuroscience 104 (2001) 467.
[24] J. Lu, D. Sherman, M. Devor, C.B. Saper, A putative flip-flop switch for control of REM sleep, Nature 441 (7093) (2006) 589–594.
[25] E. Sapin, D. Lapray, A. Berod, R. Goutagny, L. Leger, et al., Localization of the brainstem GABAergic neurons controlling paradoxical (REM) sleep, PLoS ONE 4 (2009) e4272.
[26] P.H. Luppi, D. Gervasoni, L. Verret, R. Goutagny, C. Peyron, et al., Paradoxical (REM) sleep genesis: the switch from an aminergic–cholinergic to a GABAergic–glutamatergic hypothesis, J. Physiol. Paris 100 (2006) 271.
[27] R.E. Brown, J.T. McKenna, S. Winston, R. Basheer, Y. Yanagawa, et al., Characterization of GABAergic neurons in rapid-eye-movement sleep controlling regions of the brainstem reticular formation in GAD67-green fluorescent protein knock-in mice, Eur. J. Neurosci. 27 (2008) 352.
[28] J. Lu, D. Sherman, M. Devor, C.B. Saper, A putative flip-flop switch for control of REM sleep, Nature 441 (2006) 589.
[29] T. Houben, T. Deboer, F. van Oosterhout, J.H. Meijer, Correlation with behavioral activity and rest implies circadian regulation by SCN neuronal activity levels, J. Biol. Rhythms 24 (2009) 477.
[30] J. Schaap, C.M. Pennartz, J.H. Meijer, Electrophysiology of the circadian pacemaker in mammals, Chronobiol. Int. 20 (2003) 171.
[31] M.U. Gillette, S.M. Reppert, The hypothalamic suprachiasmatic nuclei: circadian patterns of vasopressin secretion and neuronal activity in vitro, Brain Res. Bull. 19 (1987) 135.
[32] W.J. Schwartz, S.M. Reppert, S.M. Eagan, M.C. Moore-Ede, In vivo metabolic activity of the suprachiasmatic nuclei: a comparative study, Brain Res. 274 (1983) 184.
[33] M.D. Belle, C.O. Diekman, D.B. Forger, H.D. Piggins, Daily electrical silencing in the mammalian circadian clock, Science 326 (2009) 281.
[34] A. Jagota, H.O. de la Iglesia, W.J. Schwartz, Morning and evening circadian oscillations in the suprachiasmatic nucleus in vitro, Nat. Neurosci. 3 (2000) 372.
[35] J. Schaap, H. Albus, H.T. VanderLeest, P.H. Eilers, L. Detari, et al., Heterogeneity of rhythmic suprachiasmatic nucleus neurons: implications for circadian waveform and photoperiodic encoding, Proc. Natl. Acad. Sci. USA 100 (2003) 15994.
[36] C.B. Saper, T.E. Scammell, J. Lu, Hypothalamic regulation of sleep and circadian rhythms, Nature 437 (2005) 1257.
[37] X. Sun, S. Whitefield, B. Rusak, K. Semba, Electrophysiological analysis of suprachiasmatic nucleus projections to the ventrolateral preoptic area in the rat, Eur. J. Neurosci. 14 (2001) 1257.
[38] J.J. Gooley, A. Schomer, C.B. Saper, The dorsomedial hypothalamic nucleus is critical for the expression of food-entrainable circadian rhythms, Nat. Neurosci. 9 (2006) 398.
[39] G. Aston-Jones, S. Chen, Y. Zhu, M. Oshinsky, A neural circuit for circadian regulation of arousal, Nat. Neurosci. 4 (2001) 732.
[40] L.P. Morin, N. Goodless-Sanchez, L. Smale, R.Y. Moore, Projections of the suprachiasmatic nuclei, subparaventricular zone and retrochiasmatic area in the golden hamster, Neuroscience 61 (1994) 391.
[41] R.Y. Moore, J.C. Speh, GABA is the principal neurotransmitter of the circadian system, Neurosci. Lett. 150 (1993) 112.
[42] R.M. Buijs, Y.X. Hou, S. Shinn, L.P. Renaud, Ultrastructural evidence for intra- and extranuclear projections of GABAergic neurons of the suprachiasmatic nucleus, J. Comp. Neurol. 340 (1994) 381.
[43] R.M. Buijs, J. Wortel, Y.X. Hou, Colocalization of gamma-aminobutyric acid with vasopressin, vasoactive intestinal peptide, and somatostatin in the rat suprachiasmatic nucleus, J. Comp. Neurol. 358 (1995) 343.
[44] M.L. Hermes, M. Kolaj, P. Doroshenko, E. Coderre, L.P. Renaud, Effects of VPAC2 receptor activation on membrane excitability and GABAergic transmission in subparaventricular zone neurons targeted by suprachiasmatic nucleus, J. Neurophysiol. 102 (2009) 1834.
[45] S. Deurveilher, K. Semba, Indirect projections from the suprachiasmatic nucleus to major arousal-promoting cell groups in rat: implications for the circadian control of behavioural state, Neuroscience 130 (2005) 165.
[46] K. Shinohara, K. Tominaga, Y. Isobe, S.T. Inouye, Photic regulation of peptides located in the ventrolateral subdivision of the suprachiasmatic nucleus of the rat: daily variations of vasoactive intestinal polypeptide, gastrin-releasing peptide, and neuropeptide Y, J. Neurosci. 13 (1993) 793.
[47] K. Shinohara, T. Funabashi, F. Kimura, Temporal profiles of vasoactive intestinal polypeptide precursor mRNA and its receptor mRNA in the rat suprachiasmatic nucleus, Brain Res. Mol. Brain Res. 63 (1999) 262.
[48] H.E. Albers, E.G. Stopa, R.T. Zoeller, J.S. Kauer, J.C. King, et al., Day–night variation in prepro vasoactive intestinal peptide/peptide histidine isoleucine mRNA within the rat suprachiasmatic nucleus, Brain Res. Mol. Brain Res. 7 (1990) 85.
[49] T. Deboer, M.J. Vansteensel, L. Detari, J.H. Meijer, Sleep states alter activity of suprachiasmatic nucleus neurons, Nat. Neurosci. 6 (2003) 1086.
[50] R.Y. Moore, A.E. Halaris, B.E. Jones, Serotonin neurons of the midbrain raphe: ascending projections, J. Comp. Neurol. 180 (1978) 417.
[51] K.G. Bina, B. Rusak, K. Semba, Localization of cholinergic neurons in the forebrain and brainstem that project to the suprachiasmatic nucleus of the hypothalamus in rat, J. Comp. Neurol. 335 (1993) 295.
[52] C. Cajochen, Alerting effects of light, Sleep Med. Rev. 11 (2007) 453.
[53] A.A. Borbely, P. Achermann, Sleep homeostasis and models of sleep regulation, J. Biol. Rhythms 14 (1999) 557.
[54] R. Basheer, R.E. Strecker, M.M. Thakkar, R.W. McCarley, Adenosine and sleep–wake regulation, Prog. Neurobiol. 73 (2004) 379.
[55] Z.L. Huang, Y. Urade, O. Hayaishi, Prostaglandins and adenosine in the regulation of sleep and wakefulness, Curr. Opin. Pharmacol. 7 (2007) 33.
[56] T. Porkka-Heiskanen, R.E. Strecker, R.W. McCarley, Brain site-specificity of extracellular adenosine concentration changes during sleep deprivation and spontaneous sleep: an *in vivo* microdialysis study [in process citation], Neuroscience 99 (2000) 507.
[57] R. Basheer, T. Porkka-Heiskanen, D. Stenberg, R.W. McCarley, Adenosine and behavioral state control: adenosine increases c-Fos protein and AP1 binding in basal forebrain of rats, Brain Res. Mol. Brain Res. 73 (1999) 1.
[58] C.J. Van Dort, H.A. Baghdoyan, R. Lydic, Adenosine A(1) and A(2A) receptors in mouse prefrontal cortex modulate acetylcholine release and behavioral arousal, J. Neurosci. 29 (2009) 871.
[59] D.G. Rainnie, H.C. Grunze, R.W. McCarley, R.W. Greene, Adenosine inhibition of mesopontine cholinergic neurons: implications for EEG arousal, Science 263 (1994) 689.
[60] T. Porkka-Heiskanen, R.E. Strecker, M. Thakkar, A.A. Bjorkum, R.W. Greene, et al., Adenosine: a mediator of the sleep-inducing effects of prolonged wakefulness, Science 276 (1997) 1265.
[61] C.M. Portas, M. Thakkar, D.G. Rainnie, R.W. Greene, R.W. McCarley, Role of adenosine in behavioral state modulation: a microdialysis study in the freely moving cat, Neuroscience 79 (1997) 225.

[62] A.V. Kalinchuk, R.W. McCarley, D. Stenberg, T. Porkka-Heiskanen, R. Basheer, The role of cholinergic basal forebrain neurons in adenosine-mediated homeostatic control of sleep: lessons from 192 IgG-saporin lesions, Neuroscience 157 (2008) 238.
[63] Z.W. Liu, X.B. Gao, Adenosine inhibits activity of hypocretin/orexin neurons by the A1 receptor in the lateral hypothalamus: a possible sleep-promoting effect, J. Neurophysiol. 97 (2007) 837.
[64] S. Morairty, D. Rainnie, R. McCarley, R. Greene, Disinhibition of ventrolateral preoptic area sleep–active neurons by adenosine: a new mechanism for sleep promotion, Neuroscience 123 (2004) 451.
[65] N.L. Chamberlin, E. Arrigoni, T.C. Chou, T.E. Scammell, R.W. Greene, et al., Effects of adenosine on gabaergic synaptic inputs to identified ventrolateral preoptic neurons, Neuroscience 119 (2003) 913.
[66] T. Gallopin, P.H. Luppi, B. Cauli, Y. Urade, J. Rossier, et al., The endogenous somnogen adenosine excites a subset of sleep-promoting neurons via A2A receptors in the ventrolateral preoptic nucleus, Neuroscience 134 (2005) 1377.
[67] T. Sakurai, The neural circuit of orexin (hypocretin): maintaining sleep and wakefulness, Nat. Rev. Neurosci. 8 (2007) 171.
[68] A.A. Borbely, P. Achermann, Concepts and models of sleep regulation: an overview, J. Sleep Res. 1 (1992) 63.
[69] A.J. Phillips, P.A. Robinson, Sleep deprivation in a quantitative physiologically based model of the ascending arousal system, J. Theor. Biol. 255 (2008) 413.
[70] P.A. Robinson, A.J. Phillips, B.D. Fulcher, M. Puckeridge, J.A. Roberts, Quantitative modelling of sleep dynamics, Philos. Trans. A Math. Phys. Eng. Sci. 369 (2011) 3840.
[71] D.B. Forger, C.S. Peskin, A detailed predictive model of the mammalian circadian clock, Proc. Natl. Acad. Sci. USA 100 (2003) 14806.
[72] J.C. Leloup, A. Goldbeter, Toward a detailed computational model for the mammalian circadian clock, Proc. Natl. Acad. Sci. USA 100 (2003) 7051.
[73] A.J. Phillips, P.Y. Chen, P.A. Robinson, Probing the mechanisms of chronotype using quantitative modeling, J. Biol. Rhythms 25 (2010) 217.
[74] A.J. Phillips, C.A. Czeisler, E.B. Klerman, Revisiting spontaneous internal desynchrony using a quantitative model of sleep physiology, J. Biol. Rhythms 26 (2011) 441.
[75] S. Postnova, A. Layden, P.A. Robinson, A.J. Phillips, R.G. Abeysuriya, Exploring sleepiness and entrainment on permanent shift schedules in a physiologically based model, J. Biol Rhythms 27 (2012) 91.
[76] M. Nakao, A. Karashima, N. Katayama, Mathematical models of regulatory mechanisms of sleep–wake rhythms, Cell Mol. Life Sci. 64 (2007) 1236.
[77] C.G. Diniz Behn, N. Kopell, E.N. Brown, T. Mochizuki, T.E. Scammell, Delayed orexin signaling consolidates wakefulness and sleep: physiology and modeling, J. Neurophysiol. 99 (2008) 3090.
[78] M. Fleshner, V. Booth, D.B. Forger, C.G. Diniz Behn, Circadian regulation of sleep–wake behaviour in nocturnal rats requires multiple signals from suprachiasmatic nucleus, Philos. Trans. A Math. Phys. Eng. Sci. 369 (2011) 3855.
[79] C.G. Diniz Behn, V. Booth, A fast–slow analysis of the dynamics of REM sleep, SIAM J. Appl. Dyn. Syst. 11 (2012) 212.
[80] C.G. Diniz Behn, A. Ananthasubramaniam, V. Booth, Contrasting existence and robustness of REM/non-REM cycling in physiologically based models of rem sleep regulatory networks, SIAM J. Appl. Dyn. Syst. 12 (2013) 279.
[81] D.J. Kedziora, R.G. Abeysuriya, A.J. Phillips, P.A. Robinson, Physiologically based quantitative modeling of unihemispheric sleep, J. Theor. Biol. 314 (2012) 109.
[82] M. Puckeridge, B.D. Fulcher, A.J. Phillips, P.A. Robinson, Incorporation of caffeine into a quantitative model of fatigue and sleep, J. Theor. Biol. 273 (2011) 44.
[83] A.J. Phillips, P.A. Robinson, D.J. Kedziora, R.G. Abeysuriya, Mammalian sleep dynamics: how diverse features arise from a common physiological framework, PLoS Comput. Biol. 6 (2010) e1000826.
[84] B.D. Fulcher, A.J. Phillips, P.A. Robinson, Quantitative physiologically based modeling of subjective fatigue during sleep deprivation, J. Theor. Biol. 264 (2010) 407.
[85] B.D. Fulcher, A.J. Phillips, P.A. Robinson, Modeling the impact of impulsive stimuli on sleep–wake dynamics, Phys. Rev. E: Stat. Nonlinear Soft Matter Phys. 78 (2008) 051920.
[86] H.R. Wilson, J.D. Cowan, Excitatory and inhibitory interactions in localized populations of model neurons, Biophys. J. 12 (1972) 1.
[87] G. Deco, V.K. Jirsa, P.A. Robinson, M. Breakspear, K. Friston, The dynamic brain: from spiking neurons to neural masses and cortical fields, PLoS Comput. Biol. 4 (2008) e1000092.
[88] G.B. Ermentrout, D.H. Terman, Mathematical Foundations of Neuroscience, Springer, New York, 2010.
[89] H.A. Baghdoyan, R. Lydic, Neurotransmitters and neuromodulators regulating sleep, in: C. Bazil, B. Malow, M. Sammaritano (Eds.), Sleep and Epilepsy: The Clinical Spectrum, Elsevier Science, New York, 2002, pp. 17–44.
[90] F.F. De-Miguel, K. Fuxe, Extrasynaptic neurotransmission as a way of modulating neuronal functions, Front. Physiol. 3 (2012) 16.
[91] K. Fuxe, A.B. Dahlstrom, G. Jonsson, D. Marcellino, M. Guescini, et al., The discovery of central monoamine neurons gave volume transmission to the wired brain, Prog. Neurobiol. 90 (2010) 82.
[92] D. Belelli, N.L. Harrison, J. Maguire, R.L. Macdonald, M.C. Walker, et al., Extrasynaptic GABAA receptors: form, pharmacology, and function, J. Neurosci. 29 (2009) 12757.
[93] L. Descarries, V. Gisiger, M. Steriade, Diffuse transmission by acetylcholine in the CNS, Prog. Neurobiol. 53 (1997) 603.
[94] C. Morris, H. Lecar, Voltage oscillations in the barnacle giant muscle fiber, Biophys. J. 35 (1981) 193.
[95] J. Rinzel, G.B. Ermentrout, Analysis of neural excitability and oscillations, in: C. Koch, I. Segev (Eds.), Methods in Neuronal Modeling, MIT Press, Cambridge, MA, 1989.
[96] J. Clausen, E.A. Sersen, A. Lidsky, Variability of sleep measures in normal subjects, Psychophysiology 11 (1974) 509.
[97] T.R. Chay, J. Rinzel, Bursting, beating, and chaos in an excitable membrane model, Biophys. J. 47 (1985) 357.
[98] M.T. Bianchi, S.S. Cash, J. Mietus, C.K. Peng, R. Thomas, Obstructive sleep apnea alters sleep stage transition dynamics, PLoS ONE 5 (2010) e11356.
[99] R.D. Chervin, J.L. Fetterolf, D.L. Ruzicka, B.J. Thelen, J.W. Burns, Sleep stage dynamics differ between children with and without obstructive sleep apnea, Sleep 32 (2009) 1325.
[100] E.B. Klerman, W. Wang, J.F. Duffy, D.J. Dijk, C.A. Czeisler, et al., Survival analysis indicates that age-related decline in sleep continuity occurs exclusively during NREM sleep, Neurobiol. Aging 34 (2013) 309.
[101] C.G. Diniz Behn, V. Booth, A population network model of neuronal and neurotransmitter interactions regulating sleep–wake behavior in rodent species, in: A. Hutt (Ed.), Sleep and Anesthesia: Neural Correlates in Theory and Experiment, Springer, New York, 2011, pp. 107–126.
[102] S. Crochet, K. Sakai, Dopaminergic modulation of behavioral states in mesopontine tegmentum: a reverse microdialysis study in freely moving cats, Sleep 26 (2003) 801.
[103] L.D. Sanford, W.K. Hunt, R.J. Ross, A.I. Pack, A.R. Morrison, Central administration of a 5-HT2 receptor agonist and antagonist: lack of effect on rapid eye movement sleep and PGO waves, Sleep Res. Online 1 (1998) 80.
[104] A.R. Adamantidis, F. Zhang, A.M. Aravanis, K. Deisseroth, L. de Lecea, Neural substrates of awakening probed with optogenetic control of hypocretin neurons, Nature 450 (2007) 420.
[105] M.E. Carter, L. de Lecea, A. Adamantidis, Functional wiring of hypocretin and LC–NE neurons: implications for arousal, Front. Behav. Neurosci. 7 (2013) 43.
[106] S. Jego, S.D. Glasgow, C.G. Herrera, M. Ekstrand, S.J. Reed, et al., Optogenetic identification of a rapid eye movement sleep modulatory circuit in the hypothalamus, Nat. Neurosci. 16 (2013) 1637.
[107] C.C. Lo, L.A.N. Amaral, S. Havlin, P.C. Ivanov, T. Penzel, et al., Dynamics of sleep–wake transitions during sleep, Europhys. Lett. 57 (2002) 625.
[108] C.C. Lo, T. Chou, T. Penzel, T.E. Scammell, R.E. Strecker, et al., Common scale-invariant patterns of sleep–wake transitions across mammalian species, Proc. Natl. Acad. Sci. USA 101 (2004) 17545.
[109] M.S. Blumberg, C.M. Coleman, E.D. Johnson, C. Shaw, Developmental divergence of sleep–wake patterns in orexin knockout and wild-type mice, Eur. J. Neurosci. 25 (2007) 512.
[110] J. Chu-Shore, M.B. Westover, M.T. Bianchi, Power law versus exponential state transition dynamics: application to sleep–wake architecture, PLoS ONE 5 (2010) e14204.
[111] C. Blanco-Centurion, D. Gerashchenko, P.J. Shiromani, Effects of saporin-induced lesions of three arousal populations on daily levels of sleep and wake, J. Neurosci. 27 (2007) 14041.
[112] M. Sedigh-Sarvestani, S.J. Schiff, B.J. Gluckman, Reconstructing mammalian sleep dynamics with data assimilation, PLoS Comput. Biol. 8 (2012) e1002788.
[113] B.A. Lopour, S. Tasoglu, H.E. Kirsch, J.W. Sleigh, A.J. Szeri, A continuous mapping of sleep states through association of EEG with a mesoscale cortical model, J. Comput. Neurosci. 30 (2011) 471.